AD-A073 102 MITRE CORP BEDFORD MA F/G 18/3
POST-TEST ANALYSIS OF BRUNSWICK MOD SHELTER TESTED IN DICE THRO--ETC(U)
JUL 79 J M CALLIGEROS F19628-79-C-0001

UNCLASSIFIED MTR-3761 ESD-TR-79-142 NL

| OF |
ADA
073102

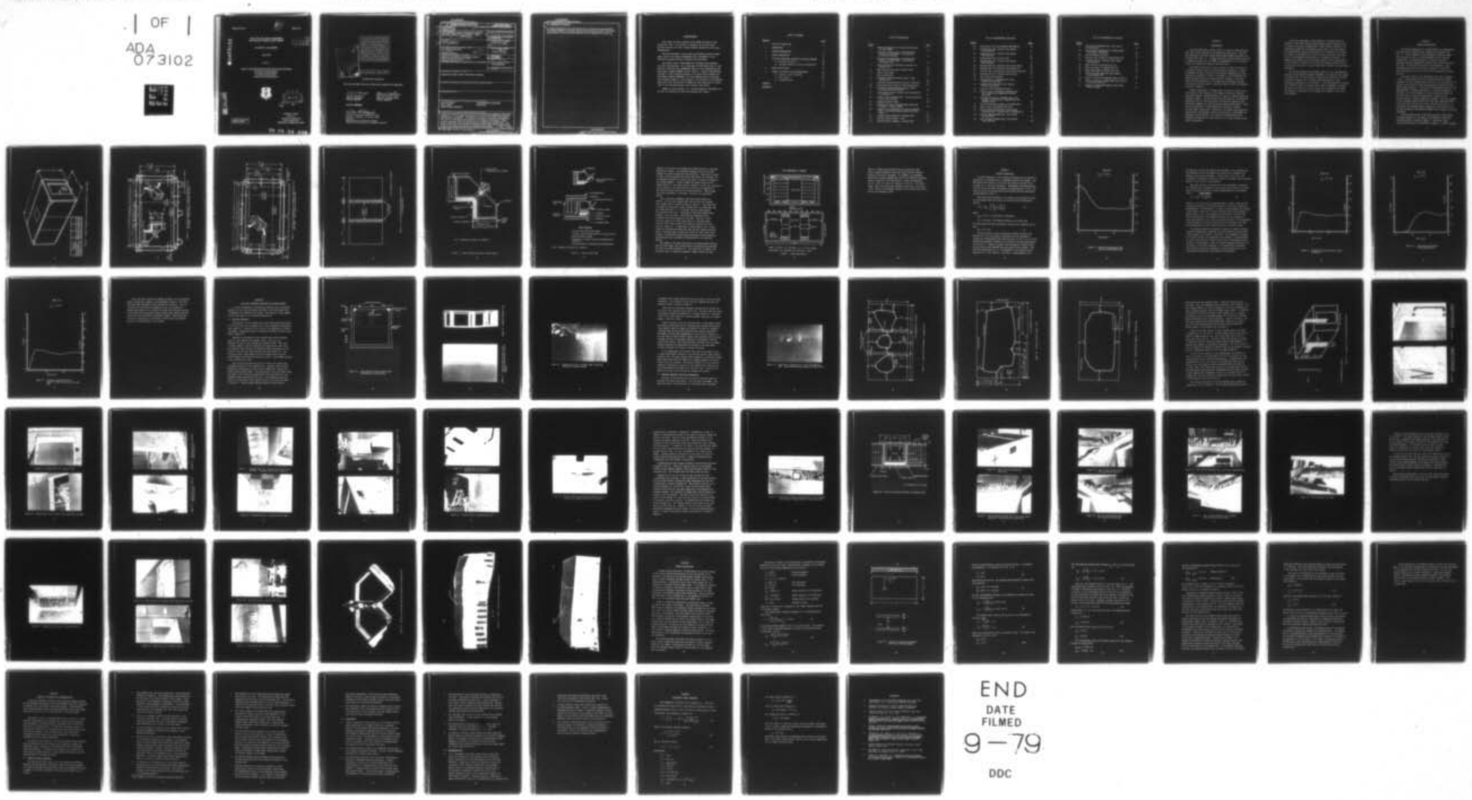

END
DATE
FILMED
9-79
DDC

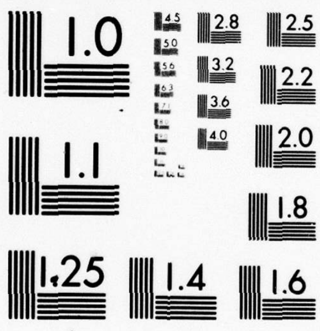

MICROCOPY RESOLUTION TEST CHART

ESD-TR-79-142

MTR-3761

LEVEL II

AD A073102

POST-TEST ANALYSIS OF BRUNSWICK MOD SHELTER TESTED IN DICE THROW

BY JOHN M. CALLIGEROS

JULY 1979

Prepared for

DEPUTY FOR SURVEILLANCE AND NAVIGATION SYSTEMS
ELECTRONIC SYSTEMS DIVISION
AIR FORCE SYSTEMS COMMAND
UNITED STATES AIR FORCE
Hanscom Air Force Base, Massachusetts

Project No. 5310
Prepared by
THE MITRE CORPORATION
Bedford, Massachusetts
Contract No. F19628-79-C-0001

REVIEW AND APPROVAL

This technical report has been reviewed and is approved for publication.

John M. Calligeros

John M. Calligeros
Project Engineer

Robert A. Karlson

Robert A. Karlson, GS-13
Project Engineer

FOR THE COMMANDER

William A. Hobgood

William A. Hobgood, Lt Colonel, USAF
Director
Environmental Surveillance Systems
Deputy for Surveillance & Navigation Systems

UNCLASSIFIED

SECURITY CLASSIFICATION OF THIS PAGE (When Data Entered)

REPORT DOCUMENTATION PAGE

19

READ INSTRUCTIONS BEFORE COMPLETING FORM

1. REPORT NUMBER
(18) ESD-TR-79-142

2. GOVT ACCESSION NO.

3. RECIPIENT'S CATALOG NUMBER

4. TITLE (and Subtitle)
(6) POST-TEST ANALYSIS OF BRUNSWICK MOD SHELTER TESTED IN DICE THROW

5. TYPE OF REPORT & PERIOD COVERED
(9) Technical rept.

6. PERFORMING ORG. REPORT NUMBER
(14) MTR-3761

7. AUTHOR(s)
(10) John M. Calligeros

8. CONTRACT OR GRANT NUMBER(s)
F19628-79-C-0001
(15)

9. PERFORMING ORGANIZATION NAME AND ADDRESS
The MITRE Corporation
P. O. Box 208
Bedford, MA 01730

(12) 78p.

10. PROGRAM ELEMENT, PROJECT, TASK AREA & WORK UNIT NUMBERS
(16) Project No. 5310

11. CONTROLLING OFFICE NAME AND ADDRESS
Deputy for Surveillance & Navigation Systems
Electronic Systems Division, AFSC
Hanscom AFB, MA 01731

12. REPORT DATE
(11) JUL [redacted]979

13. NUMBER OF PAGES
75

14. MONITORING AGENCY NAME & ADDRESS (if different from Controlling Office)

15. SECURITY CLASS. (of this report)
UNCLASSIFIED

15a. DECLASSIFICATION/DOWNGRADING SCHEDULE

16. DISTRIBUTION STATEMENT (of this Report)

Approved for public release; distribution unlimited.

17. DISTRIBUTION STATEMENT (of the abstract entered in Block 20, if different from Report)

18. SUPPLEMENTARY NOTES

19. KEY WORDS (Continue on reverse side if necessary and identify by block number)

BLAST TESTING
DICE THROW
HONEYCOMB MATERIAL
OVERPRESSURE RESPONSE
SHELTERS

20. ABSTRACT (Continue on reverse side if necessary and identify by block number)

A post-test examination and structural failure analysis of the Brunswick MOD shelter exposed to a 6.5 psi incident overpressure in the 1976 DICE THROW high explosive (HE) field test is presented. The shelter is of modular construction incorporating WR II-3/8-3.8 kraft paper honeycomb for the wall-panel core material. Shock-mounted equipment racks were located near the roadside and curbside walls. The design of the shelter was intended to withstand the blast loads and has some features that have been proposed for the GLCM communications shelter. (over)

DD FORM 1 JAN 73 1473 EDITION OF 1 NOV 65 IS OBSOLETE

UNCLASSIFIED 235 050

SECURITY CLASSIFICATION OF THIS PAGE (When Data Entered)

UNCLASSIFIED

SECURITY CLASSIFICATION OF THIS PAGE(When Data Entered)

20. **ABSTRACT (concluded)**

A detailed examination of the MOD shelter and of wall-panel sections was made. The overall condition of the shelter and the structural failure modes of the panels are described, and some recommendations for GLCM application are given.

UNCLASSIFIED

SECURITY CLASSIFICATION OF THIS PAGE(When Data Entered)

ACKNOWLEDGMENTS

This report has been prepared by The MITRE Corporation under Project No. 5310. The contract is sponsored by the Electronic Systems Division, Air Force Systems Command, Hanscom Air Force Base, Massachusetts.

The work performed in this report was directed by Major Joseph Sugg, Chief of the Shelter Management Office (ESD/OCRS) of the Electronic Systems Division at Hanscom Air Force Base.

The authors wish to acknowledge the following Army personnel for their contributions: Mr. Jules Sagui (DR SEL-LE-SS), Chief of the Shelters, Facilities and Assemblages Branch of the Communication and Electronics Command (CERCOM) and Mr. Robert A. Freiberg (CDR DEL-SA), Assistant to the Scientific Adviser of the Electronics Research and Development Command (ERADCOM), for their administrative cooperation and continuous support in every phase of the cutting-up of the shelter; Messrs. Bill Carl and Don Kaw of CERCOM for their many hours of assistance in the data-gathering at Fort Monmouth, New Jersey.

Thanks are also extended to Lt. Steven Penaskovic (ESD/OCRS) for his help in obtaining the data and analyzing the results.

TABLE OF CONTENTS

LIST OF ILLUSTRATIONS

LIST OF ILLUSTRATIONS (Continued)

LIST OF ILLUSTRATIONS (Concluded)

SECTION 1

INTRODUCTION

The DICE THROW event was the fifth in a series of high-explosive (HE) field tests conducted by the Defense Nuclear Agency. The test was conducted at the White Sands Missile Range (WSMR), New Mexico, on 6 October 1976 (Ref. 1). A charge consisting of approximately 628 tons of ammonium nitrate fuel oil (ANFO), corresponding to a 1 KT nuclear yield, was detonated to generate the blast wave.

The primary objectives of the test were to study the effects of a simulated nuclear blast on various military equipment, to assess the damage incurred, evaluate the operational vulnerability of the systems, and establish a level of confidence in the theoretical and empirical methods used for predicting blast response. This data could provide information for survivability/vulnerability design criteria of tactical systems, including Command, Control and Communication (C^3) shelters.

Several operational C^3 systems which utilize the S-280 and the S-250 shelters were fielded in DICE THROW. In addition, some non-operational shelter configurations were tested to evaluate design and hardness concepts. One such shelter was fabricated by the Brunswick Corporation and its testing involved collaboration among the Army Electronics Command, the Army Ballistics Research Laboratories (BRL), and the Directorate of Civil Engineering, Electronic Systems Division (ESD), Hanscom AFB. Because of its modular paper-honeycomb construction, the Brunswick shelter construction for DICE THROW was designated the MOD shelter. The design of the MOD shelter was intended to withstand the blast effects of a 7.3-psi incident (free-field) overpressure.

A post-test assessment of the condition of the MOD shelter is relevant to the Ground Launched Cruise Missile (GLCM) program because of certain structural considerations. These include, primarily, the similarity between the core-design concept used for the wall panels in the MOD shelter and the one proposed by a contractor for the GLCM LCC shelter, and similarities in the location, isolation, and connection of the equipment racks relative to the shelter structure. In addition, the condition of the Brunswick shelter after being exposed to the weather for a period of two years following the blast test is relevant from the point of view of materials, sealants, and fabrication techniques.

The authors examined the Brunswick shelter at the Communications Research and Development Command (CORADCOM), Fort Monmouth, New Jersey, in January 1979, for the purpose of assessing the incurred structural response and damage, and to resolve some uncertainties in the structural construction of the shelter. A plan was devised for cutting up the shelter walls at the Sheet Metal Shop at CORADCOM, structural specimens were removed for detail study, and photographs were taken. The purpose of this report is to present the findings of this post-test analysis.

SECTION 2

SHELTER CONFIGURATION

The exterior dimensions of the MOD shelter are approximately the same as the S-280 electronic communication shelter (see Fig. 1). The wall panels of the MOD embody a structural sandwich construction with a 3-inch honeycomb core and aluminum facing sheets. A water-resistant structural kraft-paper honeycomb material designated by Hexcel as WR 11-3/8-3.8 Shelter Core (Ref. 2) was used for the panel core throughout. This honeycomb has a 3/8-inch cell size, a density of 3.8 lb/ft^3, and was developed for use in various air-transportable military shelters.

Structural details of the MOD shelter are shown in Figures 2 and 3. Each roadside wall core facing (inside and outside) consisted of three aluminum sheets 0.10 inch thick connected by two vertical splice strips located approximately 48 inches from the shelter ends (Figure 4). Splicing was necessitated because of the unavailability of large-sized sheets of 0.10 inch thickness at the time. Since the roadside wall would receive the impact of the shock wave, vertical extrusions were riveted at each splice location to provide additional strength. The panel facings for the remaining shelter walls were made from continuous sheets 0.063 inch thick and did not include stiffening extrusions. It is believed that 5052-H34 sheet aluminum was used throughout for the facing material, and 6061-T6 aluminum for the edge and vertical extrusions.

Cross-sectional views of the edge extrusions, which served as framing members for the shelter, and details of the panel-joining geometry are shown in Figure 5. Additional panel constructional details are depicted in Figure 6. As seen in these

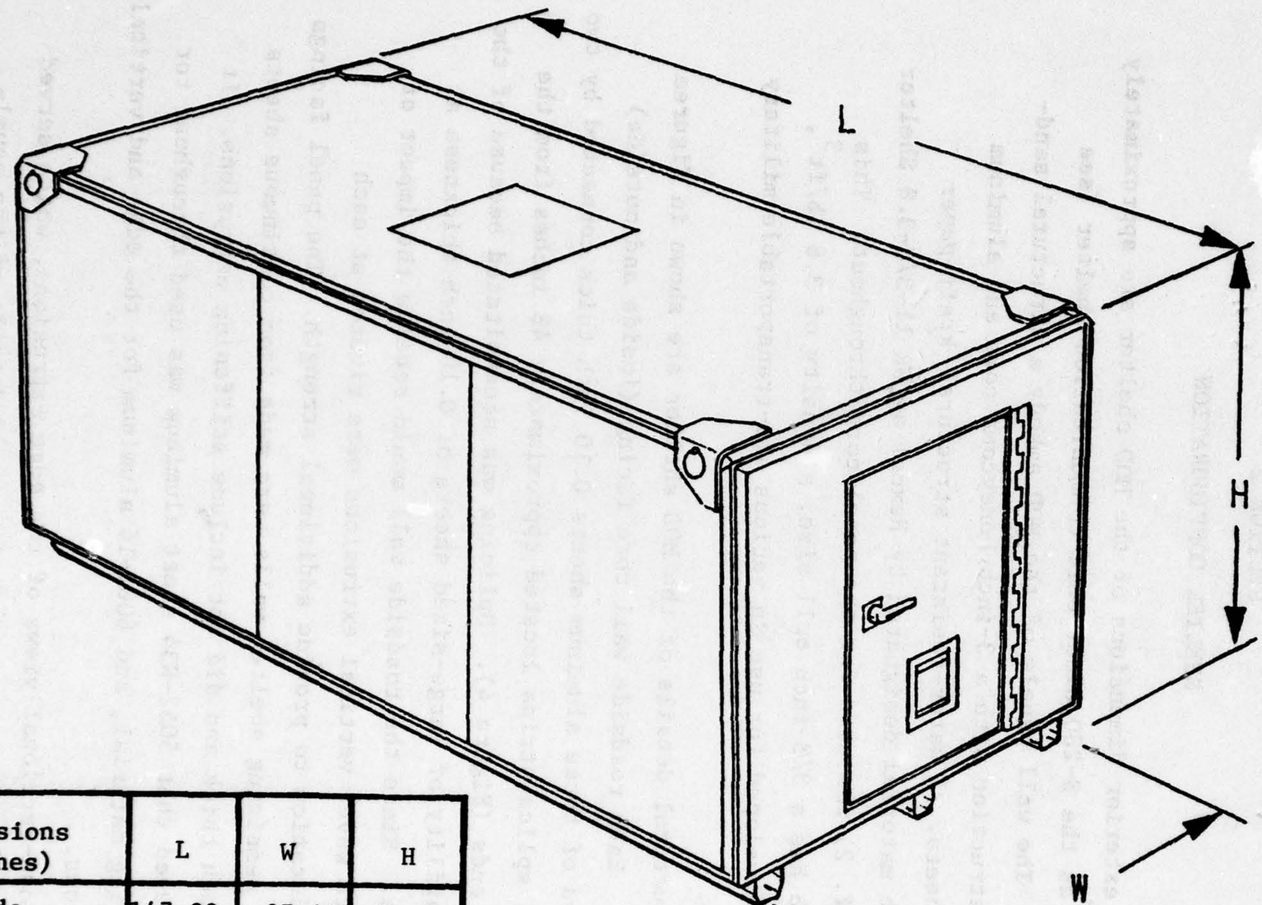

Dimensions (inches)	L	W	H
Max Outside	147.00	87.00	83.38
Inside, ± 1/8	136.00	80.70	73.10

Figure 1. Exterior Dimensions of Brunswick MOD Shelter for DICE THROW

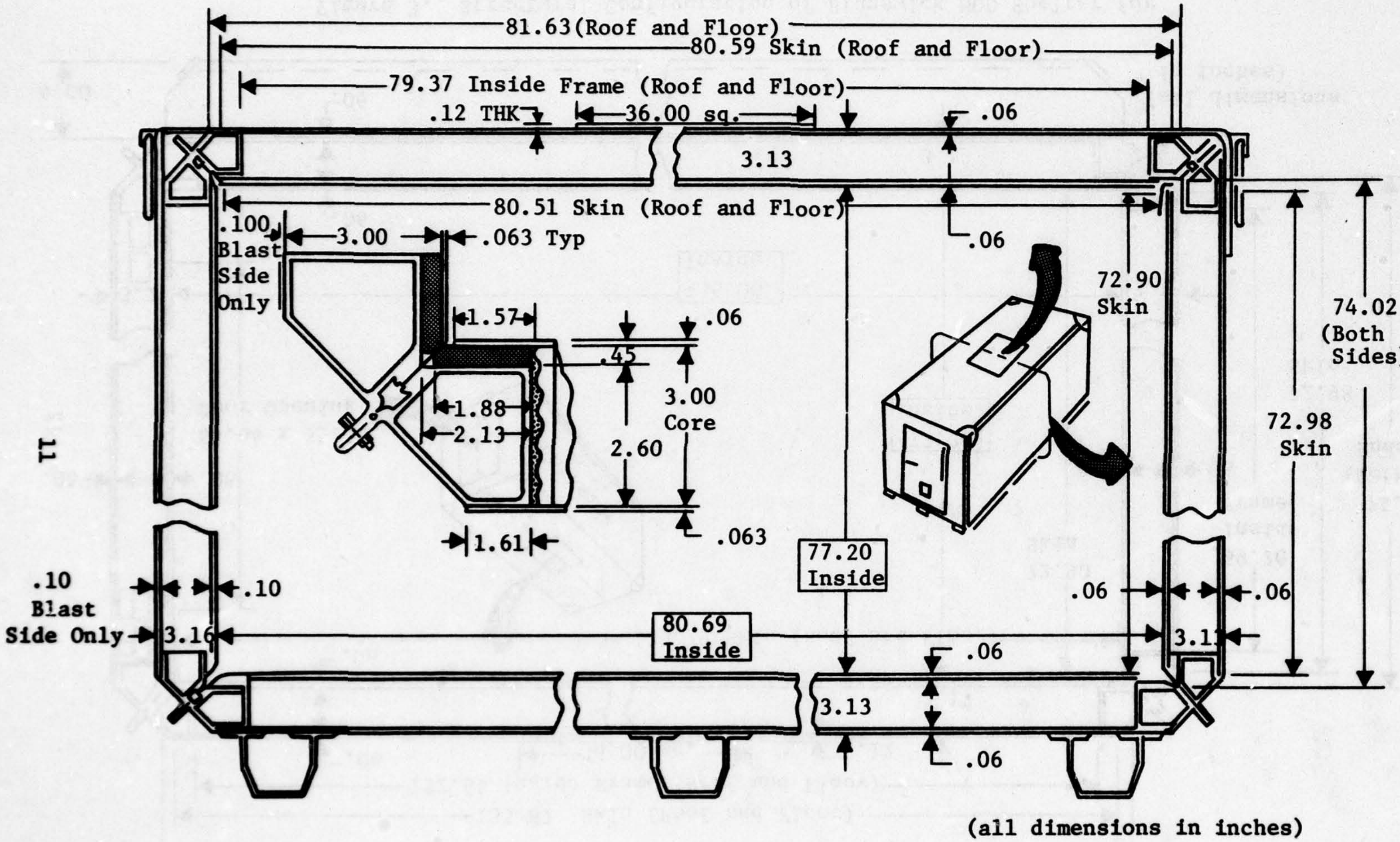

Figure 2. Structural Configuration of Brunswick MOD Shelter for DICE THROW - View Looking at the Door End Wall.

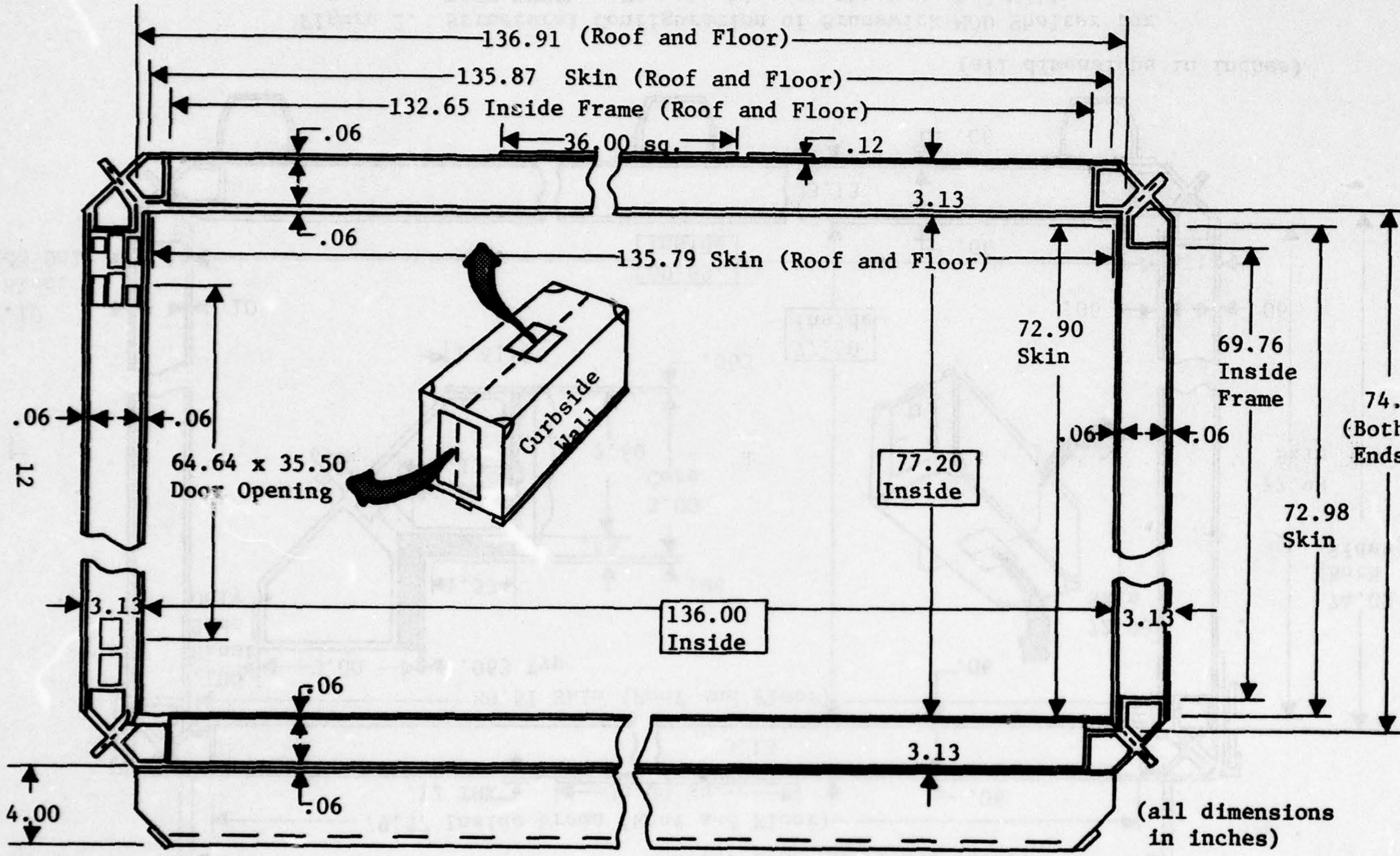

Figure 3. Structural Configuration of Brunswick MOD Shelter for DICE THROW - View Looking at Curbside Wall

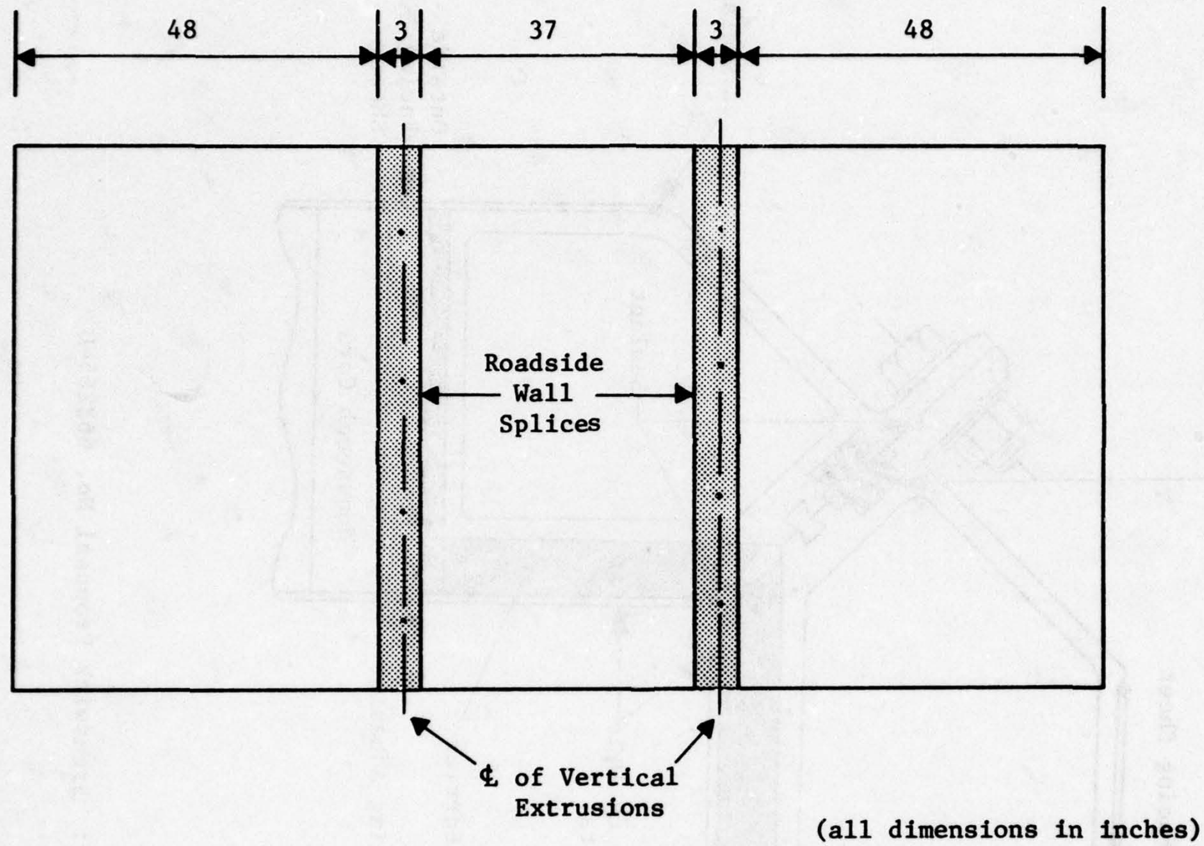

Figure 4. Splice and Vertical Extrusion Locations For Roadside Wall

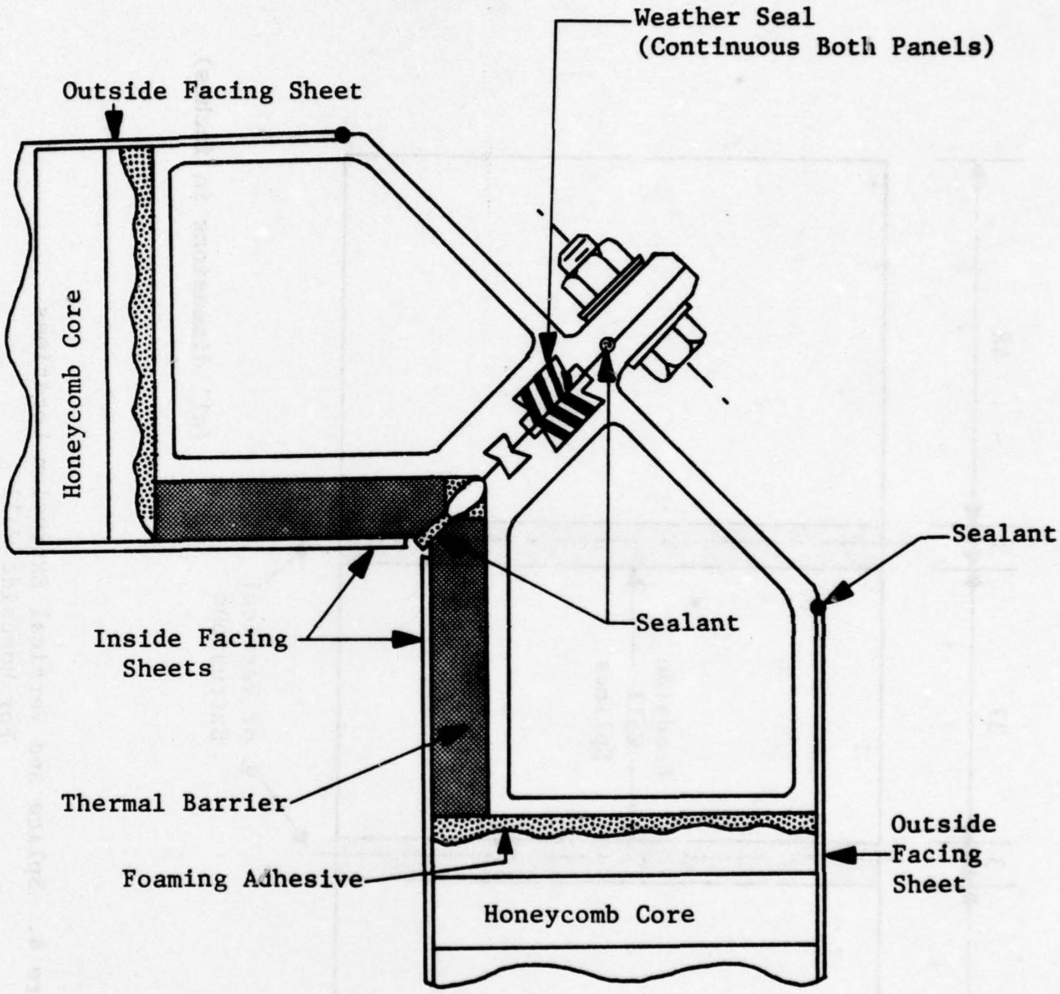

Ref: Brunswick Proposal No. 662265-0

Figure 5. Edge Extrusion and Panel Joining Detail

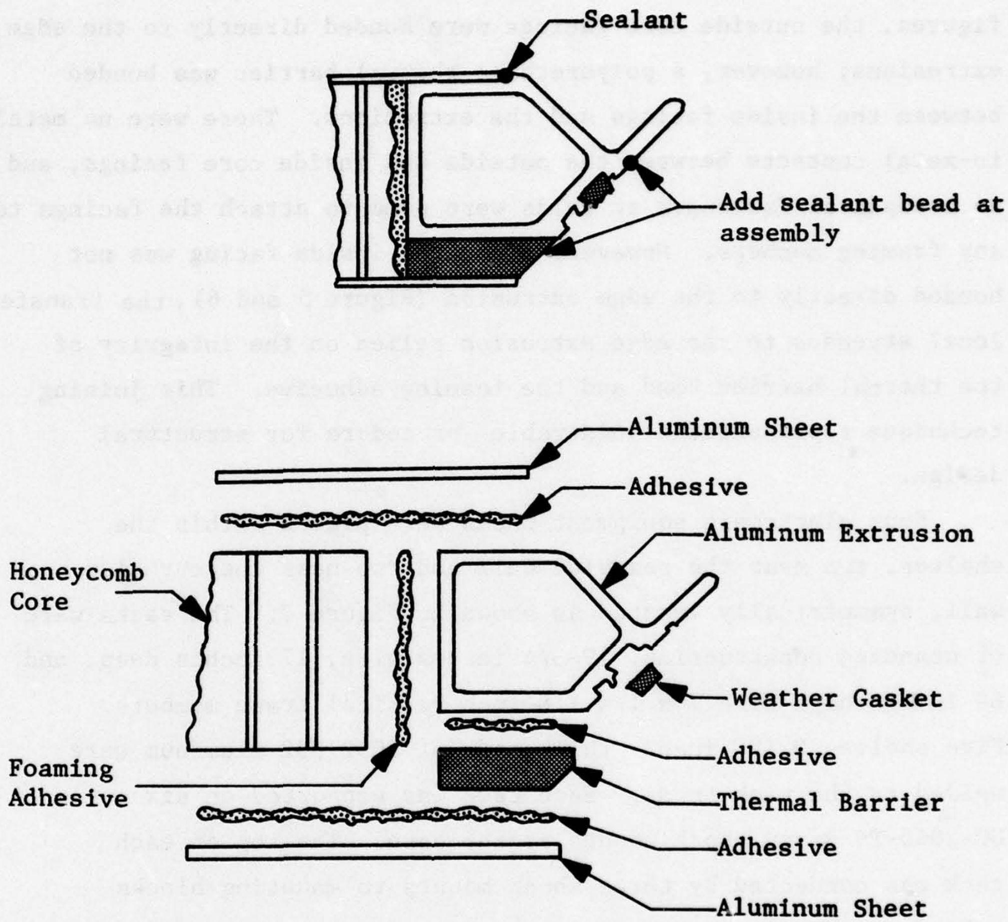

Panel Elements

- Protects and Seals Panel Edges
- Provides Self-Aligning Method of Joining Panels
- Retains Weather Gasket
- Provides for Modular Construction/Knock-Down Capability
- Isolates Metallic Components/No Through Metal

Ref: Brunswick Proposal No. 662265-0

Figure 6. Typical Panel Edge

figures, the outside core facings were bonded directly to the edge extrusions; however, a polyurethane thermal barrier was bonded between the inside facings and the extrusions. There were no metal-to-metal contacts between the outside and inside core facings, and no mechanical fasteners or welds were used to attach the facings to any framing members. However, since the inside facing was not bonded directly to the edge extrusion (Figure 5 and 6), the transfer of local stresses to the edge extrusion relied on the integrity of the thermal barrier bond and the foaming adhesive. This joining technique represented a vulnerable procedure for structural design.

Four electronic equipment racks were placed within the shelter, two near the roadside wall and two near the curbside wall, symmetrically located as shown in Figure 7. The racks were of standard construction, 19-3/4 inches wide, 17 inches deep, and 69 inches high with 1 x 1 x 1/8-inch vertical frame members. Five shelves 0.190 inch thick made of 5052 H32 aluminum were welded to the rack frame. Each rack was supported on six UC-2060-T6 Barry shock mounts at the base. The top of each rack was connected by three shock mounts to mounting blocks bolted to the corner formed by the adjacent vertical wall and the roof (Figure 7). A separation of approximately two to three inches was maintained between the racks and the adjacent vertical walls to preclude impact between the walls and racks under blast loading. Conceptually similar shock-mounting and wall-separation configurations were proposed by GTE/Sylvania for the GLCM LCC shelter.

The weight of the empty MOD shelter was approximately 1928 lb, and the total weight with racks and shock mounting plates was 2300 lb; each rack frame weighed 55 lb. The racks did not support any electronic gear or simulated equipment weights during the test.

(all dimensions in inches)

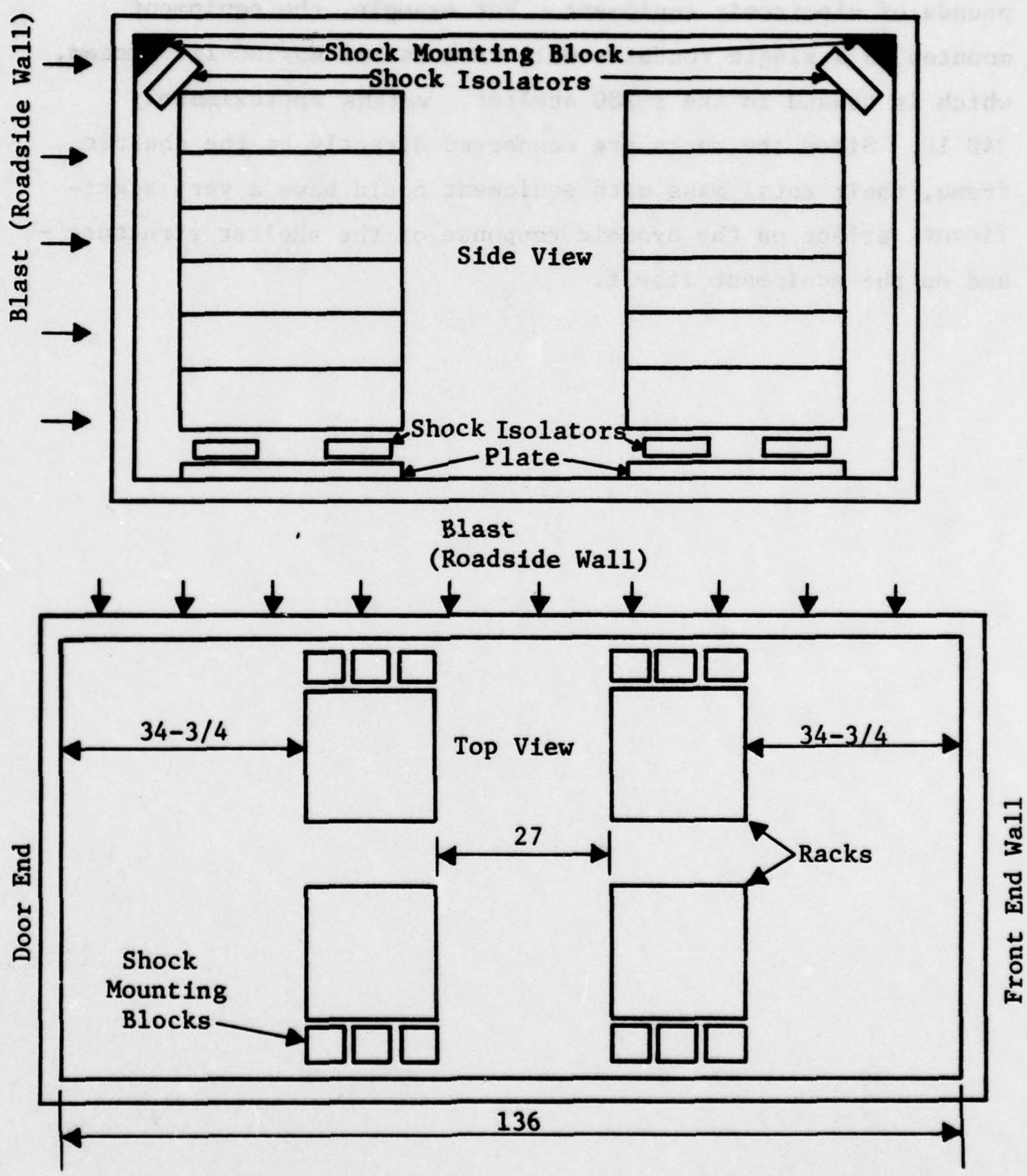

Racks - 19-3/4 x 17 x 69 with 1 x 1 x 1/8 Al Tubing

Rack Shelf (5) 5052 H32 Al 0.190 inch thick

Figure 7. Rack Installation

This is a significant deviation from an operational mode where a single equipment rack could contain several hundred pounds of electronic equipment. For example, the equipment mounted on a single roadside wall rack in the AN/TRC-117 system, which is housed in the S-280 shelter, weighs approximately 340 lb. Since the racks are connected directly to the shelter frame, their total mass with equipment could have a very significant effect on the dynamic response of the shelter structure - and on the equipment itself.

SECTION 3

LOADING DESCRIPTION

A brief description of the loading experienced by the shelter is appropriate in assessing the corresponding response and damage. The MOD shelter was located at the blast line where an incident overpressure of 7.3 psi was anticipated. Measurements indicated, however, that the actual incident overpressure was approximately 6.5 psi, the same as for one of two BRL-retrofitted shelters and the operational system AN/TRC-117 (Ref. 1).

The reflected overpressure Δp_r acting on the roadside wall hit by the incident shock wave may be calculated from the expression (Ref.3)

$$\Delta p_r = 2p_{s_o} \left[\frac{4p_{s_o} + 7p_o}{p_{s_o} + 7p_o} \right] \qquad (1)$$

where

p_{s_o} = 6.5 psi = the incident overpressure

p_o = 12.58 psi = the ambient pressure at the test site

The calculated reflected overpressure acting on the roadside wall is thus

$$\Delta p_r = 15.7 \text{ psi} \qquad (2)$$

The time history of the overpressure loadings acting on the shelter for a 6.5 psi incident overpressure may be estimated by scaling the corresponding time histories given in Ref. 4 for a 6.0-psi incident overpressure originally calculated by the BAAL hydrodynamic code of Ref. 5. Figure 8 presents the overpressure loading acting at the center of the roadside wall, calculated in this manner. Note that the overpressure at t = 0 corresponds to the reflected overpressure of 15.7 psi from Eq. 2 and that, at approximately 10-15

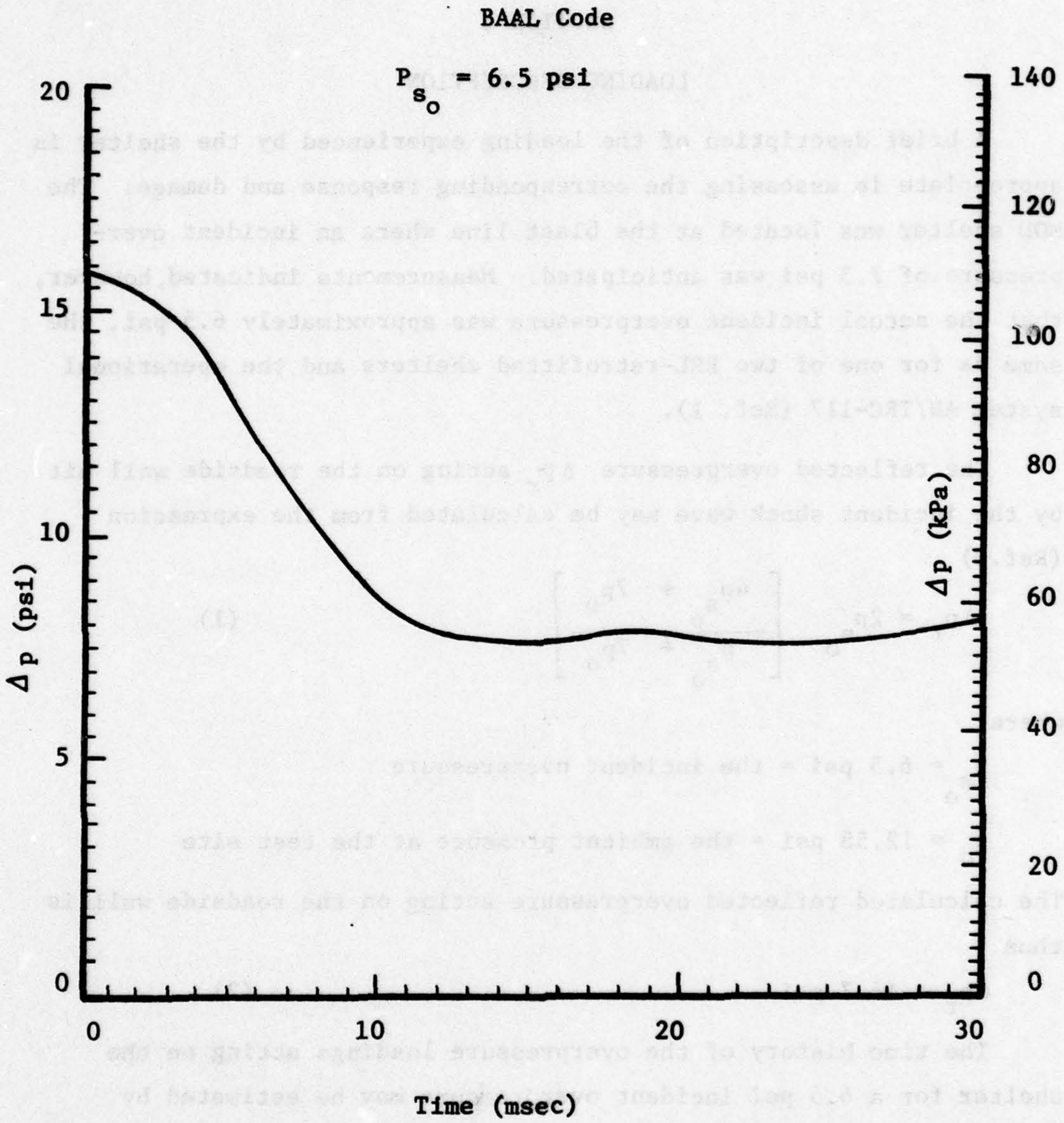

Figure 8. Estimated Overpressure Near Center of MOD Roadside Wall

milliseconds, diffractive effects have subsided at the roadside wall. The overpressure near the edges of the wall will be somewhat less because of the rarefaction waves. At the center of the roof, the calculated overpressure is given in Figure 9, reaching a peak of approximately 7.0 psi at about 5 milliseconds.

The time required for initiation of the overpressure loading on the curbside wall is dependent on the shock front velocity, V_s, which may be calculated from the following Rankine-Hugoniot relationship (Ref. 3)

$$V_s = c_o \sqrt{\frac{7p_o + 6p_{s_o}}{7p_o}} \qquad (3)$$

where c_o = 1117 ft/sec is the ambient speed of sound. With the calculated shock speed of 1342 ft/sec from Eq. 3, the time required is approximately 5.4 milliseconds. At about 16 milliseconds, the loading at the center of the roof is fully developed (Fig. 10) attaining a peak of about 7 psi. The loadings at the centers of the door end and front end walls are presented in Figure 11, also peaking to a level approximately 7 psi. As with the roadside wall, the overpressure along the edges of the other walls will also be somewhat less than the overpressures at their centers because of rarefaction waves.

The suddenly applied overpressure loading will excite the panel structural frequencies, resulting in dynamic deflections and accelerations normal to the plane of the panel. The fundamental frequency of the panel motion, as calculated in the Appendix, is approximately 78 cps for the roof and curbside walls, with a corresponding period of about 13 milliseconds. Since the higher-frequency modes will also contribute to the panel response, it is conservatively estimated that the total structural responses of the wall panels due to the overpressure loading will peak within 50 milliseconds.

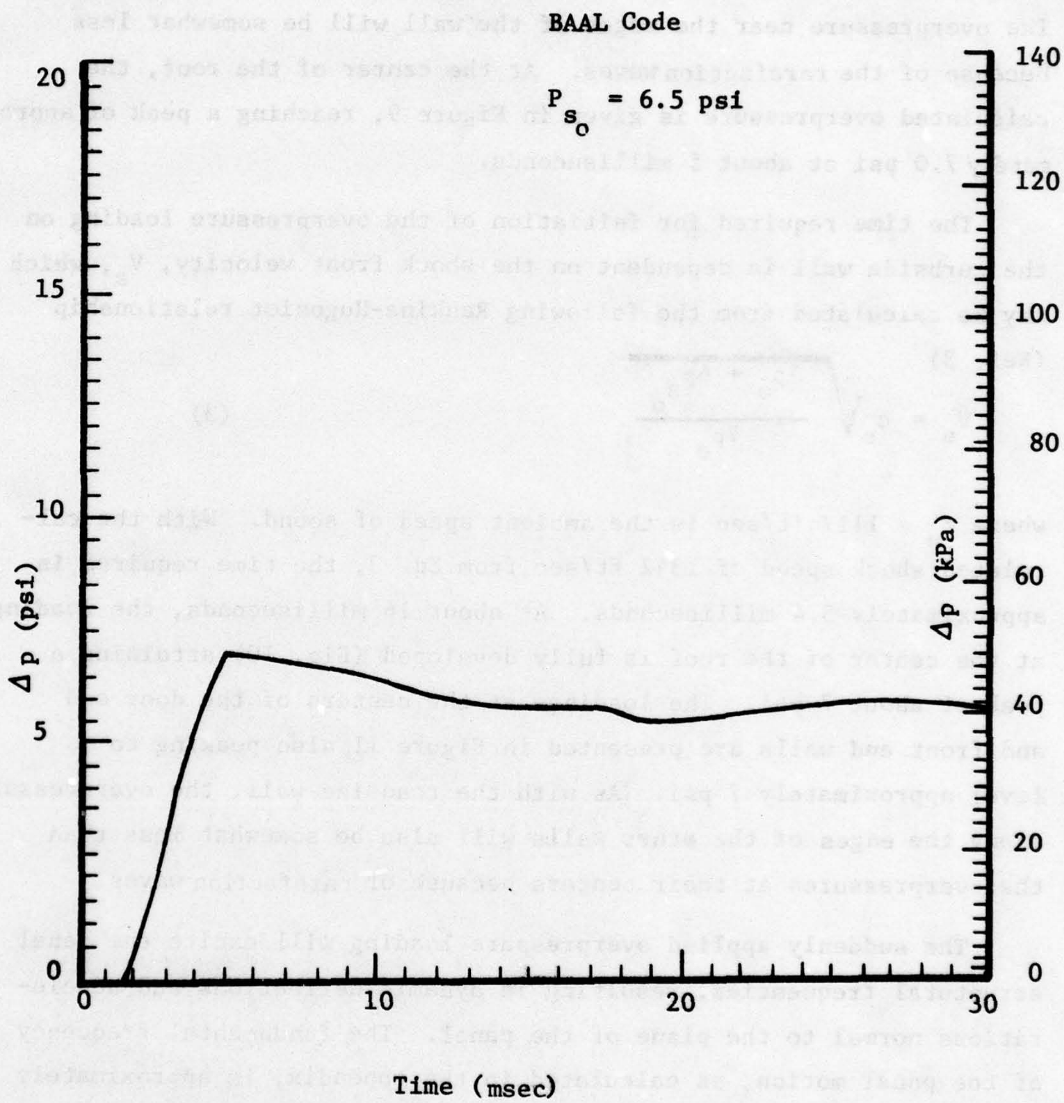

Figure 9. Estimated Overpressure Near Center of MOD Roof

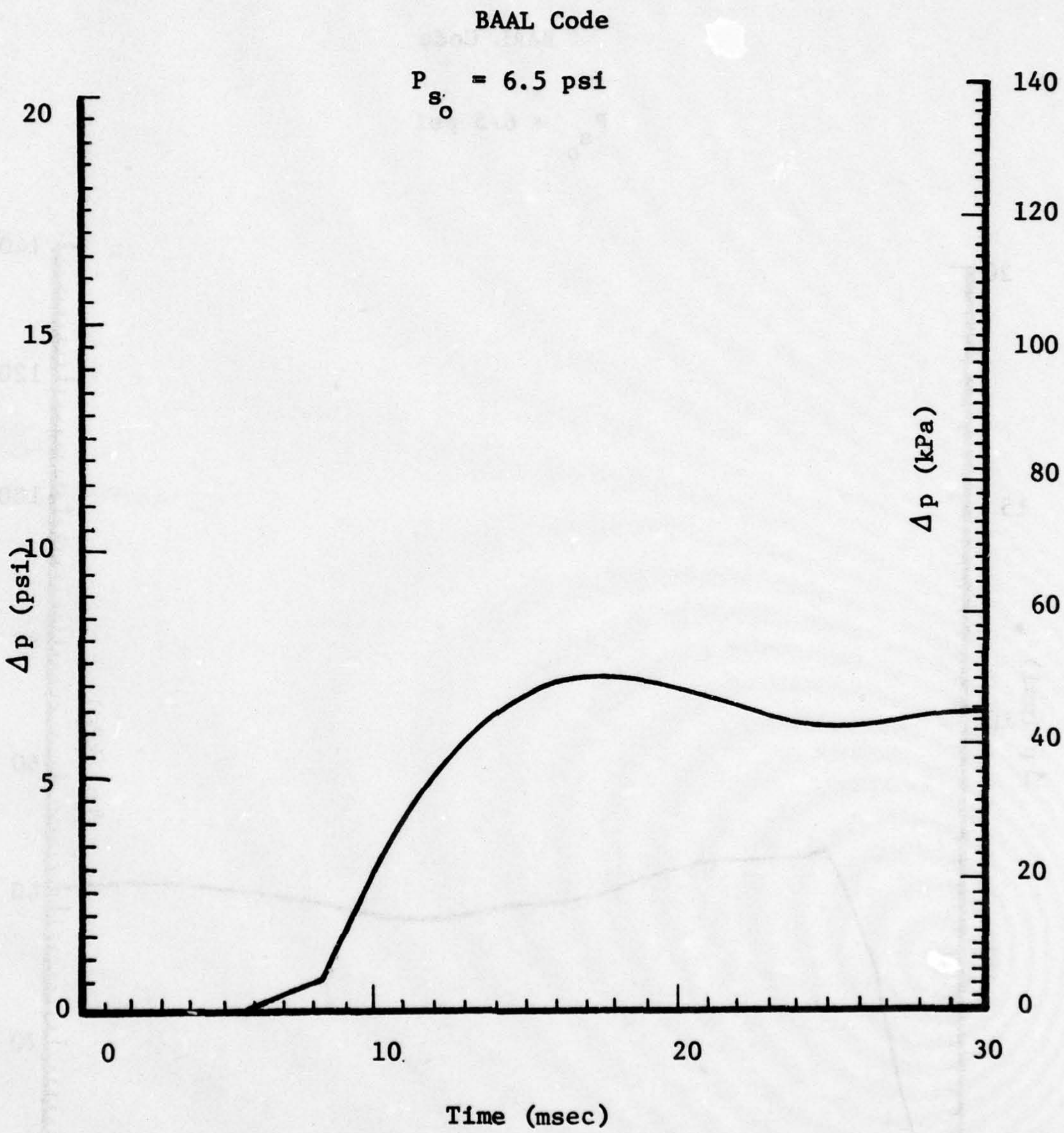

Figure 10. Overpressure Near Center of MOD Curbside Wall

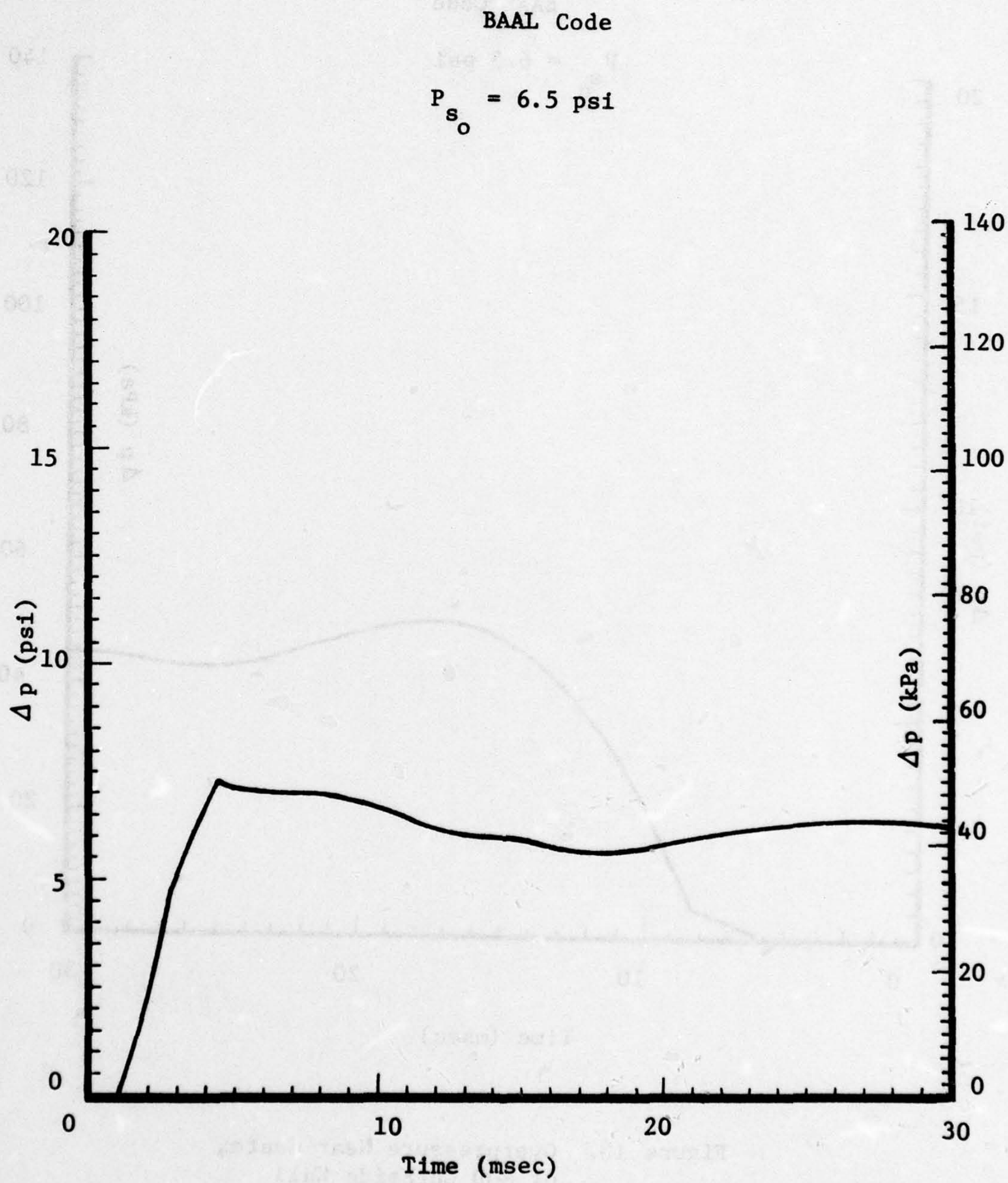

Figure 11. Estimated Overpressure Near Center of MOD Front End and Door End Wall

After the panel structural responses subside, the truck-mounted shelter system will respond to the drag-phase loading of the blast, exciting large rigid-body rolling motions of the system. This is a result of the low natural frequency of the truck suspension system, whose motion is excited by the large positive-phase duration of the blast wave (a duration roughly twenty times greater than the duration of the diffractive overpressure phase). This rigid body motion will peak within a few seconds, as was seen in the motion pictures of the MOD shelter truck system.

SECTION 4

POST-TEST STRUCTURAL CONDITION OF THE MOD SHELTER

A careful examination of the shelter exterior and of structural sections cut out from the shelter was made at the Sheet Metal Shop of CORADCOM, Fort Monmouth, New Jersey. The results of this examination are discussed in the following subsections.

4.1 Exterior Condition

The exterior of the roadside wall, which had received the impact of the shock wave, had a permanent bi-concave (dished-in) deformation (see Figure 12). Several of the rivets on the roadside wall splices had popped, causing the splices to separate partially from the facing sheets (Figure 13).

Imprints on the inside of the roadside wall surface indicated that the wall impacted the adjacent racks. The roof also impacted the tops of the curbside and roadside racks. There were no signs, however, that the curbside wall impacted the rear racks. The roadside racks received noticeable permanent deformations, particularly the rack near the front-end wall (see Figure 14). The vertical upright frame members were bent significantly and some welds between the shelves and frame had cracked. Less damage occurred to the curbside wall racks.

The roof and curbside walls did not display the concave-like deformation pattern of the roadside wall. Instead, these surfaces exhibited large depressions near the wall edges with a large flat-shaped region between edges. The deformation in the roof began along the edges of the isolator mounting blocks that were bolted to the lengthwise edge extrusions of the roof. The depression along the edge and the flatness of the central portion of the roof are shown in Figure 15. Had the upper mounting blocks not been present,

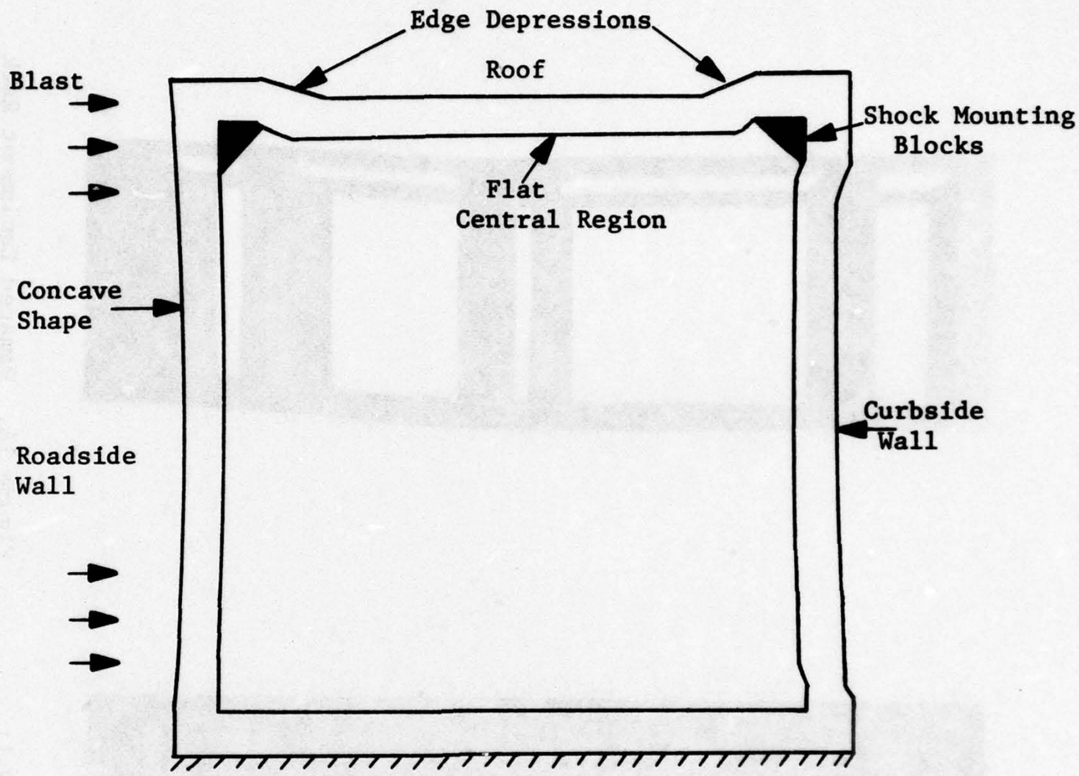

Figure 12. Cross-Section View of Shelter Wall Deformations at Mid-Section

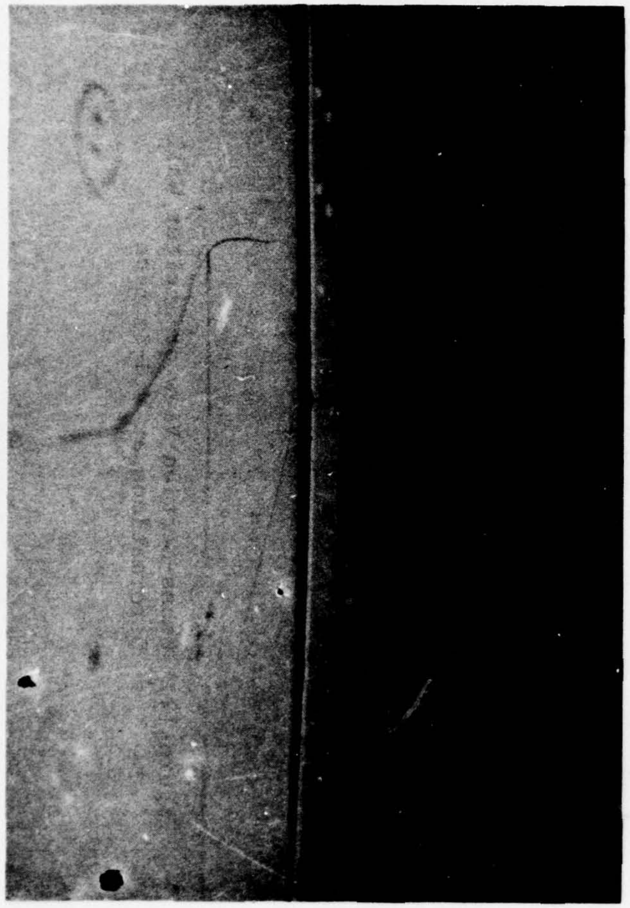

Figure 13. Interior View, Roadside Wall. Splice Separation Due to Rivet Failure

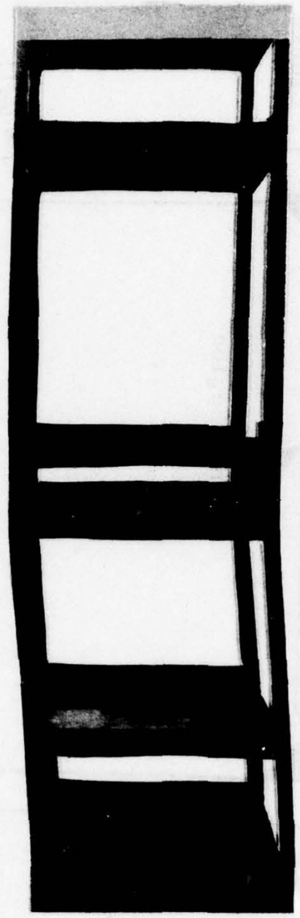

Figure 14. Damaged Equipment Rack

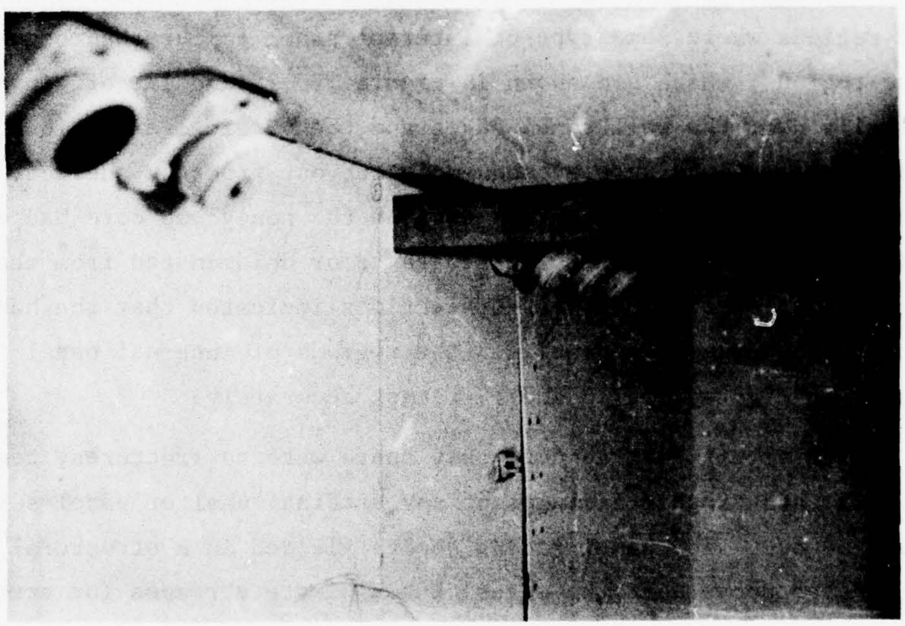

Figure 15. Depression of Roof, Straight Edge Indicating Flatness of Central Region

deformation most likely would have occurred closer to the roof edge extrusions. The condition of the roof and roadside wall near the mounting blocks is shown in Figure 16.

There were no noticeable permanent deformations in either the door end or the opposite (front-end) walls. Nor were there any signs of permanent bending deformations of any edge extrusion. The epoxy filler in the door frame had cracked; however, there was no visible damage to the door frame.

Careful tapping of the wall surfaces with a light hammer identified regions where some type of internal panel failure had occurred. These regions, which are shown in Figures 17, 18 and 19, originated typically near the wall panel edges and the vertical extrusions. When panel sections were subsequently cut out from the shelter, it was seen that in these "failed" regions the honeycomb core had either ruptured in shear or otherwise separated or delaminated from the panel facing sheets. The cut-up sections indicated that the hammer-tapping technique had identified the regions of internal panel failure in Figures 17, 18 and 19 rather accurately.

It is significant to note that there were no fractures, tears, or other catastrophic failures of any external shelter panel surface, inside or out. The panel facing sheets yielded in a structural sense, where noted above near the edges, but ultimate stresses (or strain levels) were not exceeded. The shelter appeared to be in very good condition, displaying no effects of the weather after being in the field approximately two years after the blast test. There were no signs of any water entry through the damaged wall panels.

4.2 Detailed Internal Structural Examination

Sections 12-inches wide were cut from the MOD wall panels to ascertain the nature and extent of the internal core damage. The cuts were made at the mid-section of the shelter since the panel

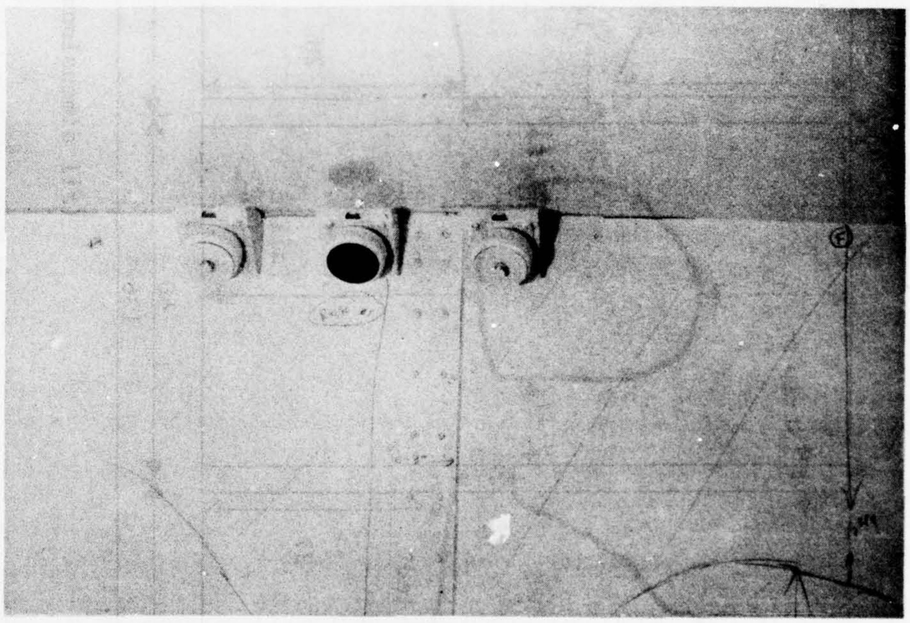

Figure 16. Condition of Intersection of Roof and Roadside Wall. Upper Shock Mounting Blocks and Wall Splice

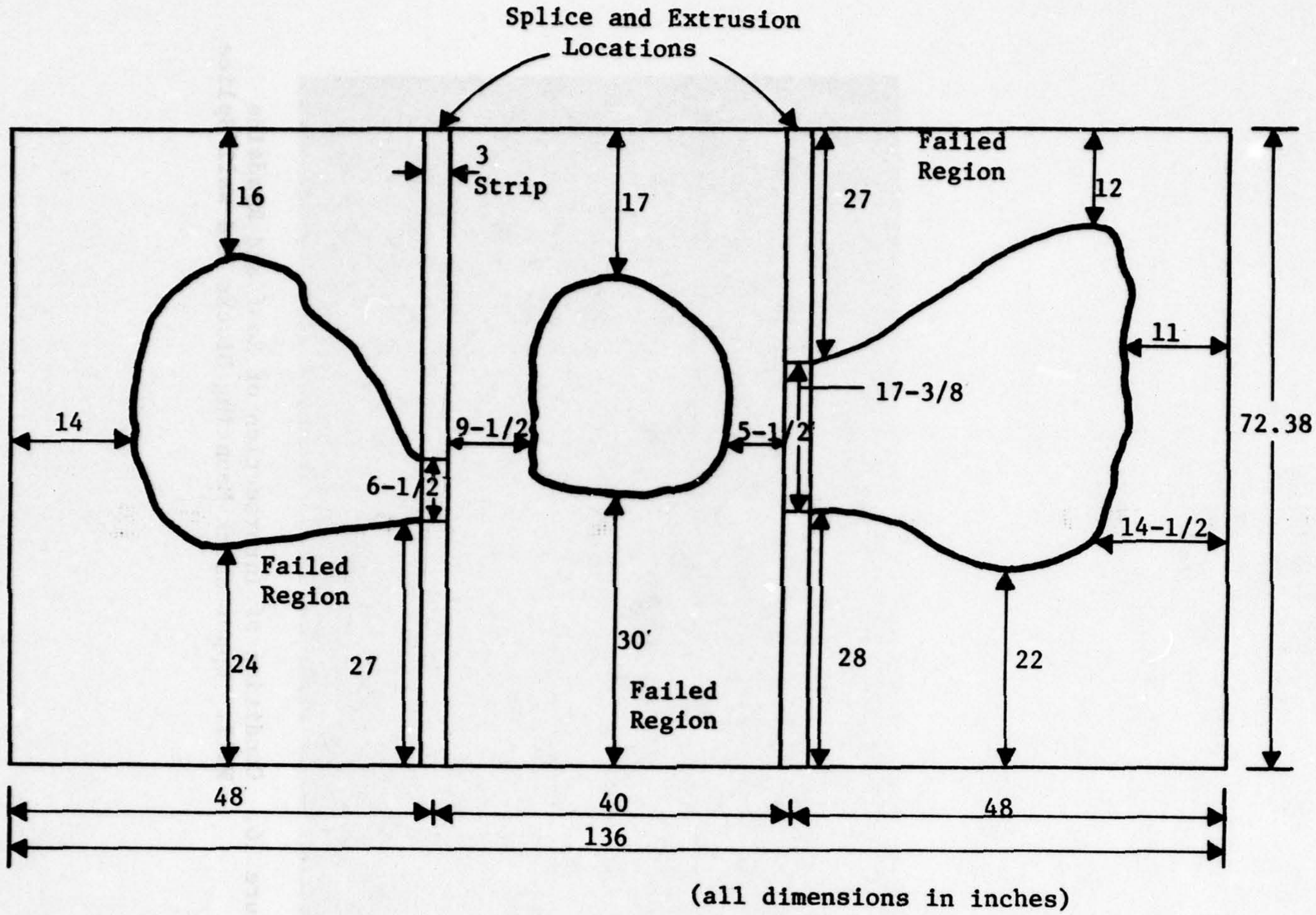

Figure 17. Internal Failure Regions - Roadside Wall

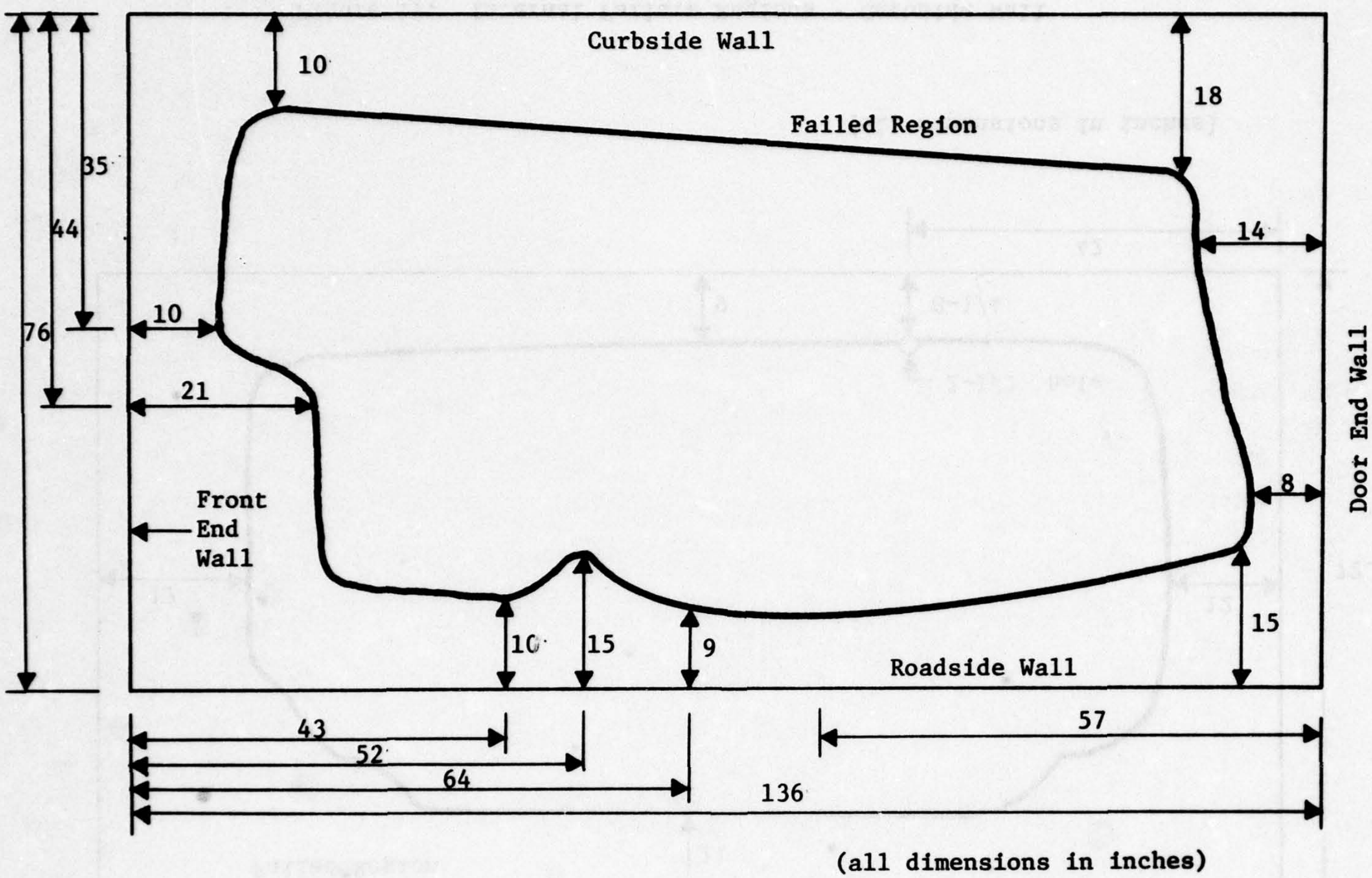

Figure 18. Internal Failure Region - Roof

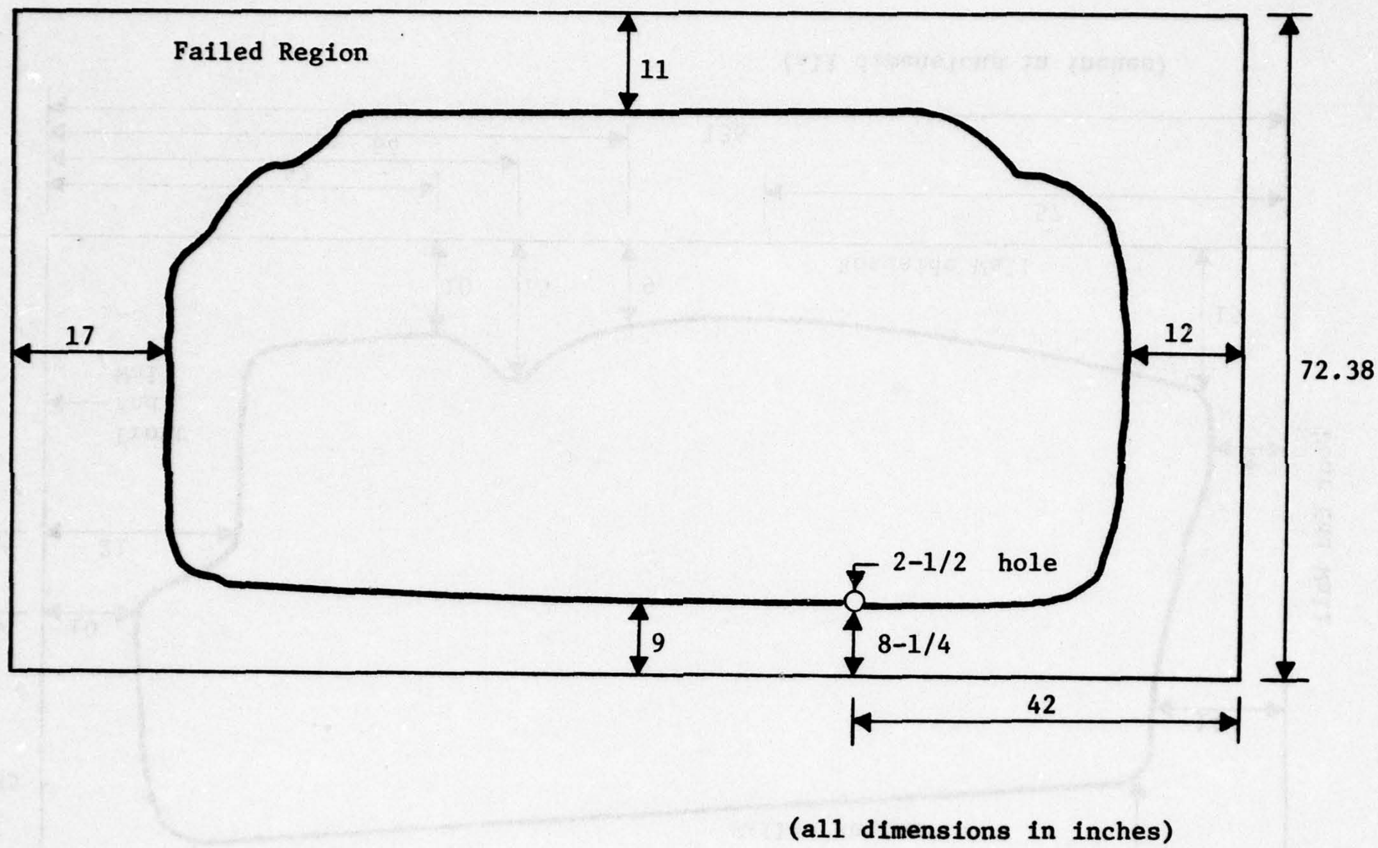

Figure 19. Internal Failure Regions - Curbside Wall

deformations were the greatest there. Figure 20 illustrates the cuts made. The cuts extended across the widths of the roadside, roof, and curbside panels, as close as possible to the edge extrusions, so that continuous sections could be examined edge-to-edge. In addition, a horizontal 27-inch cut was made in the roadside wall to confirm the presence (and any surrounding damage) of the vertical stiffener, which was unknown at the time of the test. A router was used to cut the metal facings since it was feared that a saber saw or similar such tool would inadvertently pull the skin from the honeycomb. Though tedious, this procedure was successful.

Views of the upper portion of the roadside wall-cut are shown in Figures 21, 22, 23, and 24. Internal panel failure occurred as a result of shear failure of the core on the right side of the cut and at the top of the cut. The shear failure is distinctly visible in Figures 22 and 24, running in planes that are approximately 45 degrees with respect to the plane of the panel. The core failure at the top (Figure 23) extends the width of the cut and probably continues along a considerable portion of the roof edge extrusion.

At the top left portion of the roadside-wall cut (Figure 21) and at the sides of the base (Figures 25, 26, 27 and 28), the core had separated from the outside facing sheets. In some places, this separation was due to core failure at the adhesive surface since parts of the core material remained imbedded within the adhesive. In other areas, the adhesive had failed at the facing sheet surface. The delaminated region extended considerably from the base extrusion on the roadside wall (Figures 25 and 26). At the base of the cut (Figure 28), the core fractured by shear over its full width, similar to the failure at the top of the cut.

The 27-inch horizontal cut in the roadside wall is shown in Figures 29, 30, 31, 32 and 33. The concave-like deflection of the

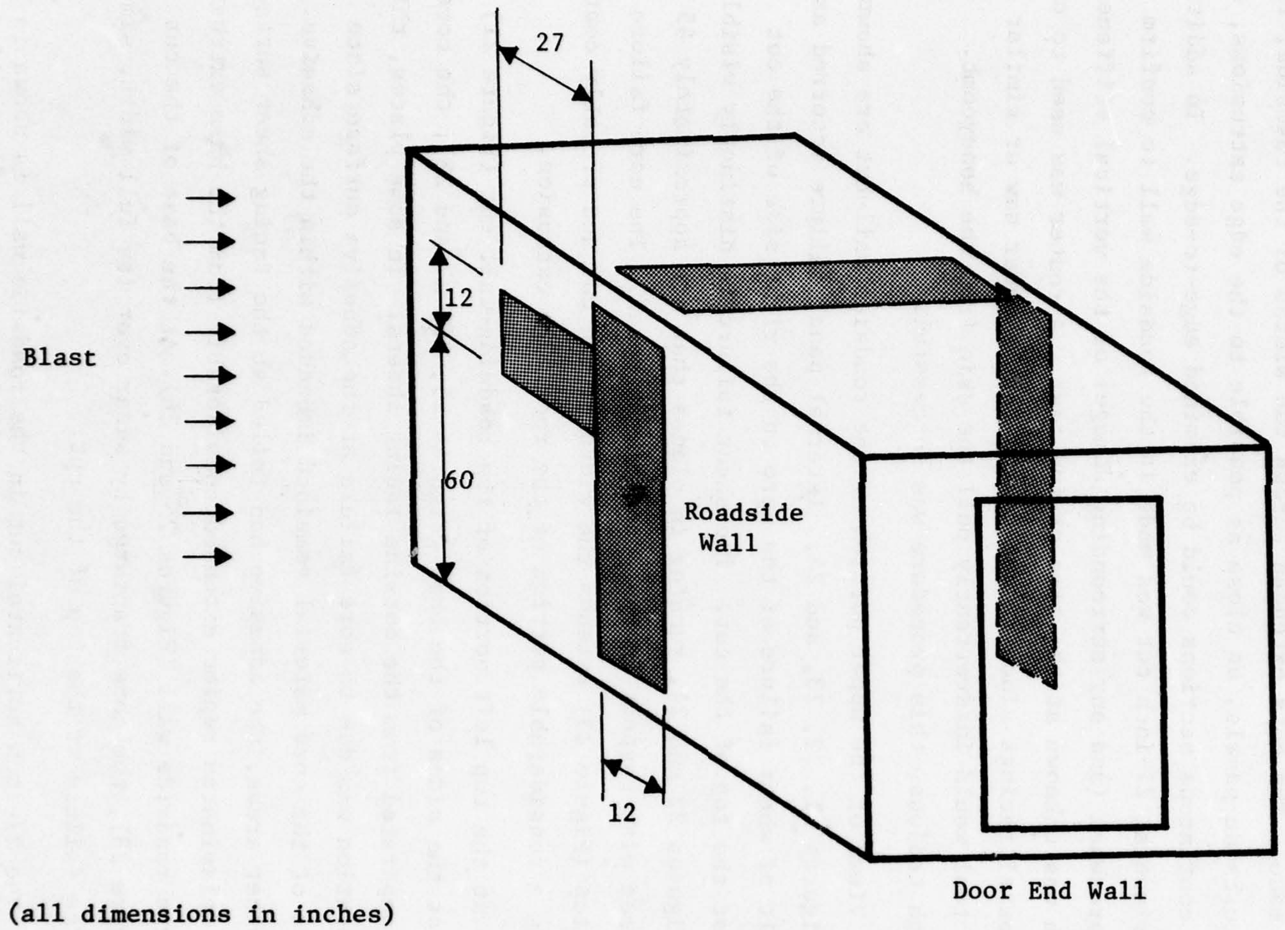

Figure 20. Sections Cut Out from Brunswick MOD Shelter

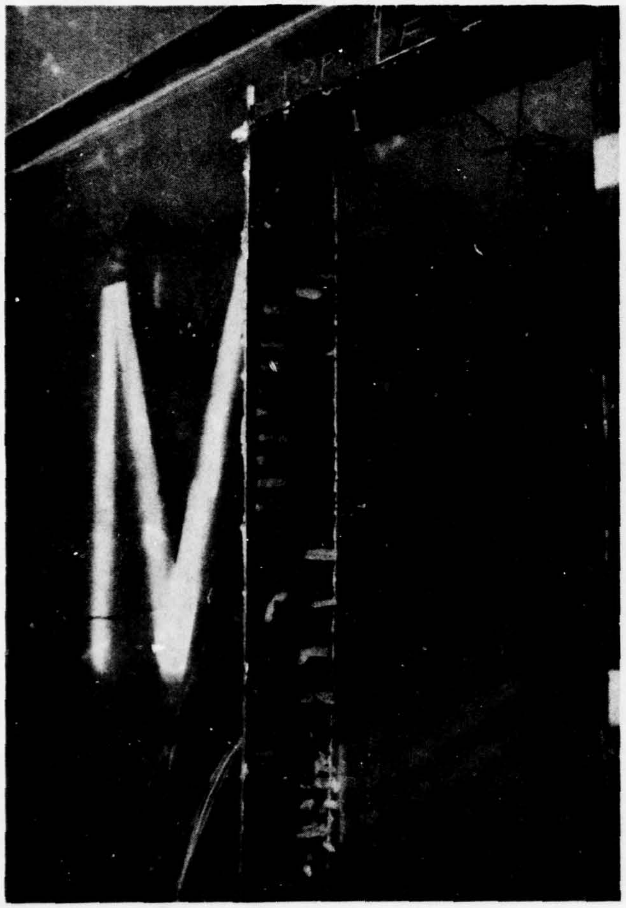

Figure 21. Roadside Wall Cut, Exterior View Toward Front End Wall

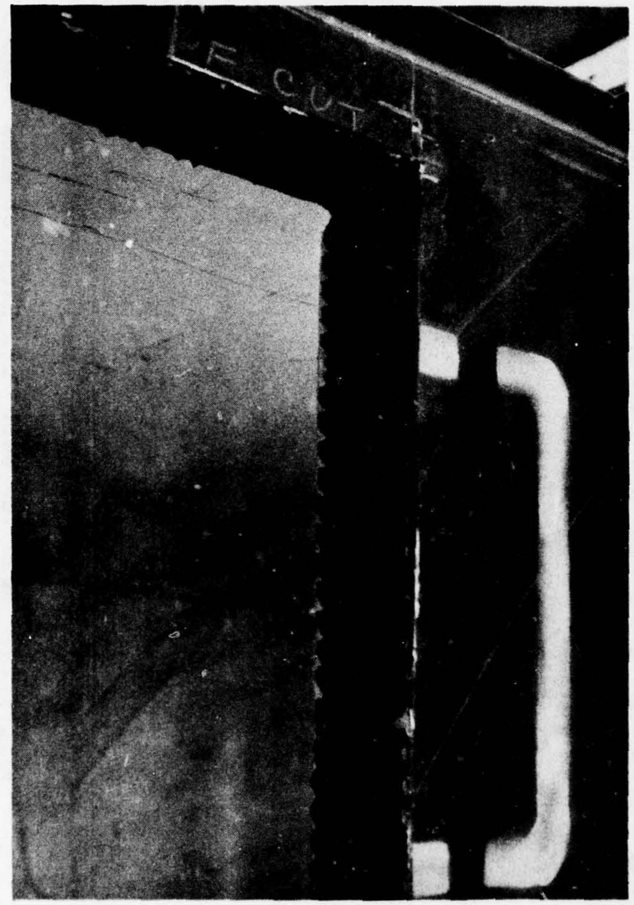

Figure 22. Roadside Wall Cut, Exterior View Toward Door End Wall

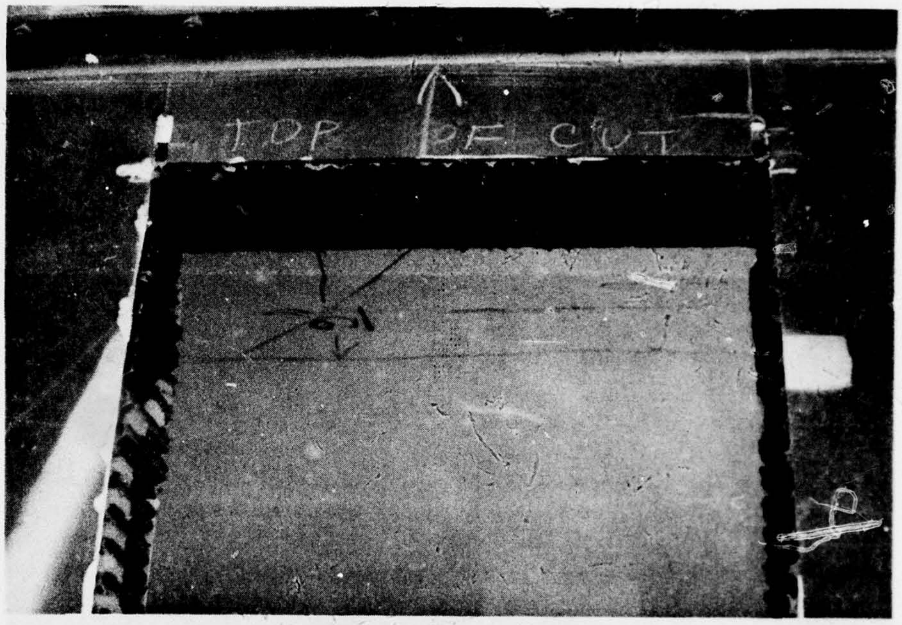

Figure 23. Roadside Wall Cut, Exterior View

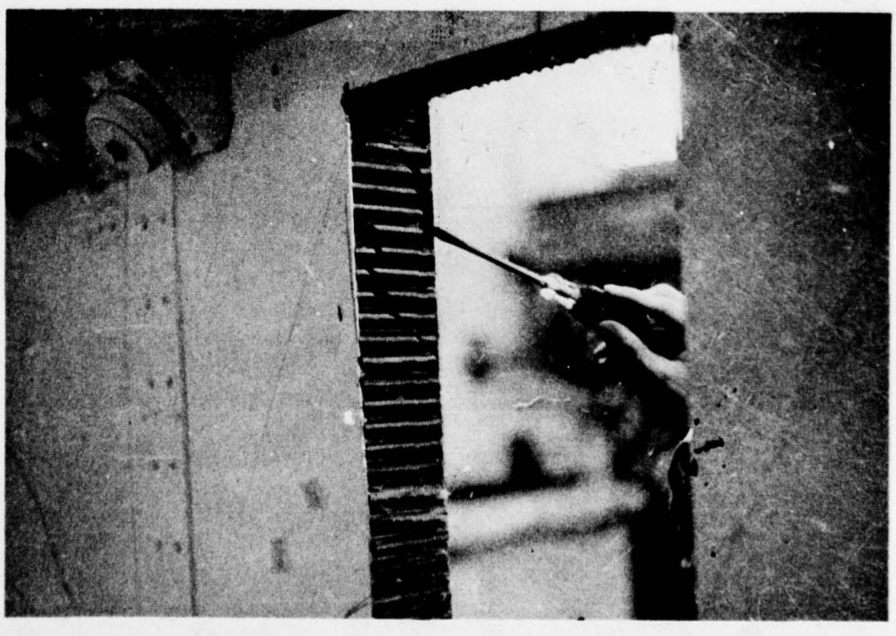

Figure 24. Roadside Wall Cut, Interior View Toward Door End Wall

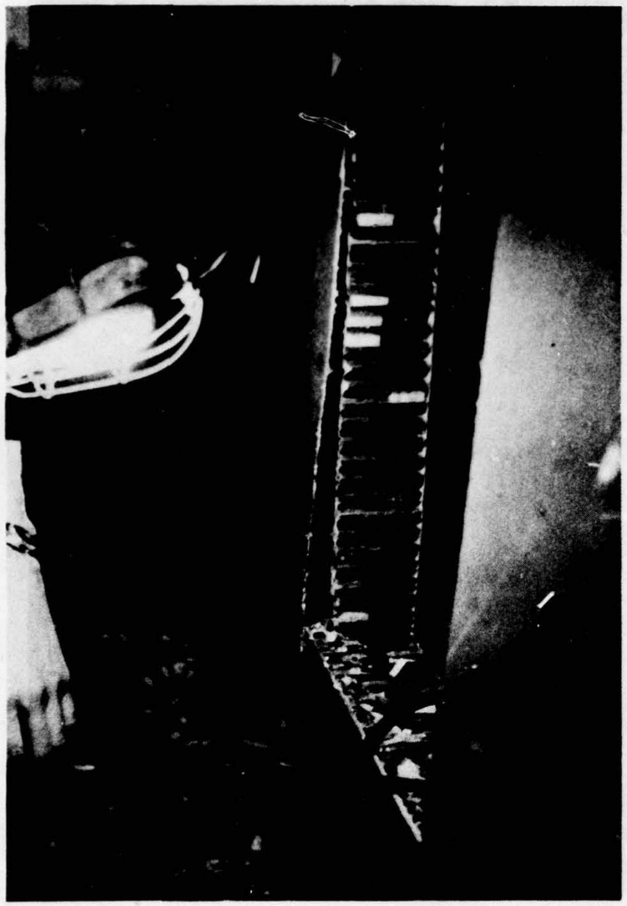

Figure 25. Roadside Wall Cut, Exterior View Toward Front

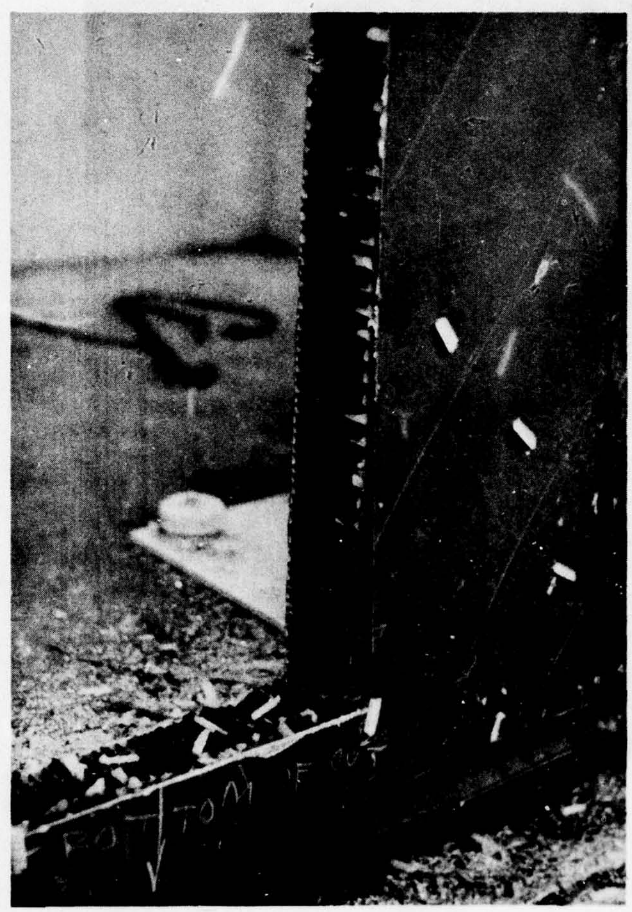

Figure 26. Roadside Wall Cut, Exterior View Toward Door

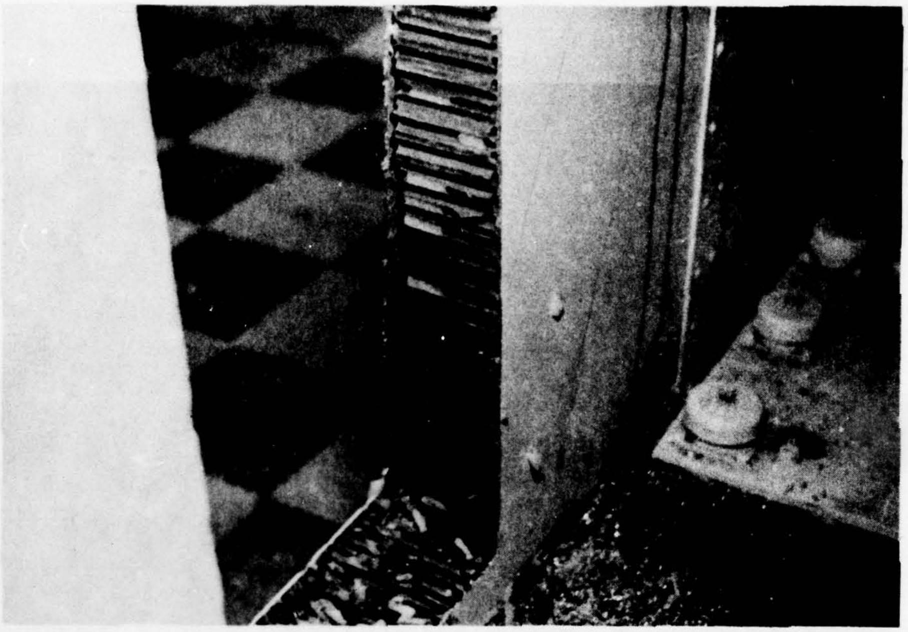

Figure 27. Roadside Wall Cut, Interior View Toward Front End Wall. Equipment Rack Shock Isolators

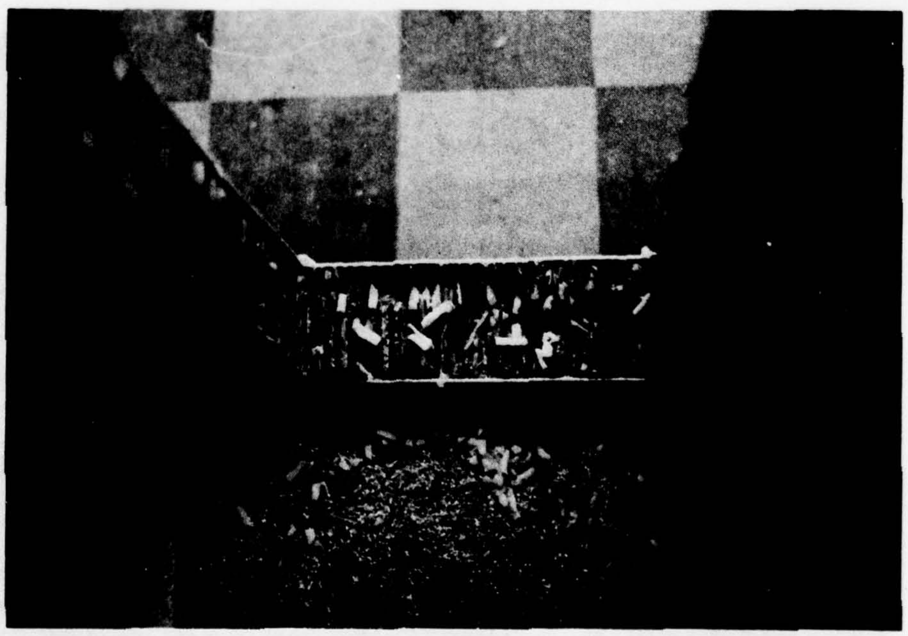

Figure 28. Roadside Wall Cut, Interior View of Base

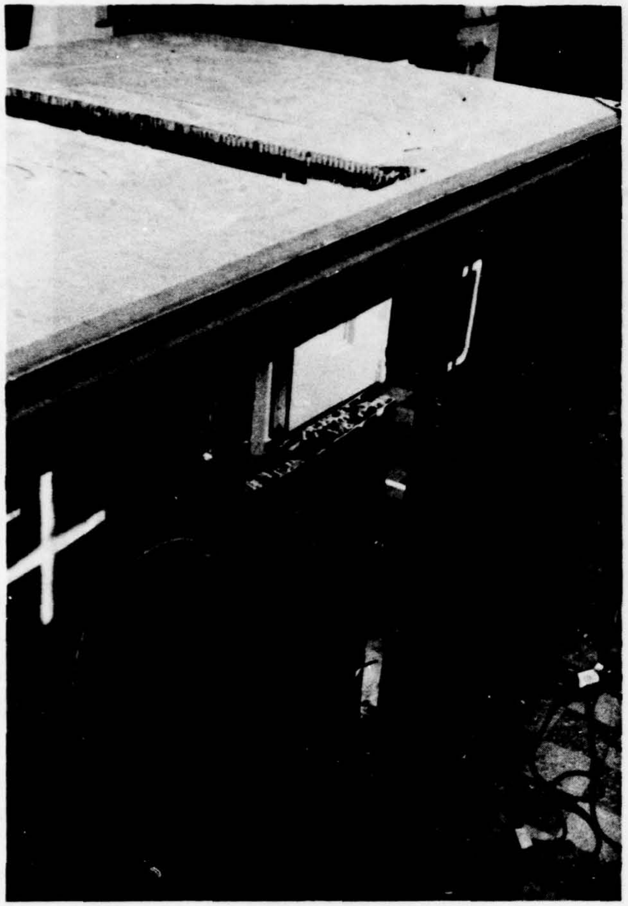

Figure 29. View Toward Door End Wall

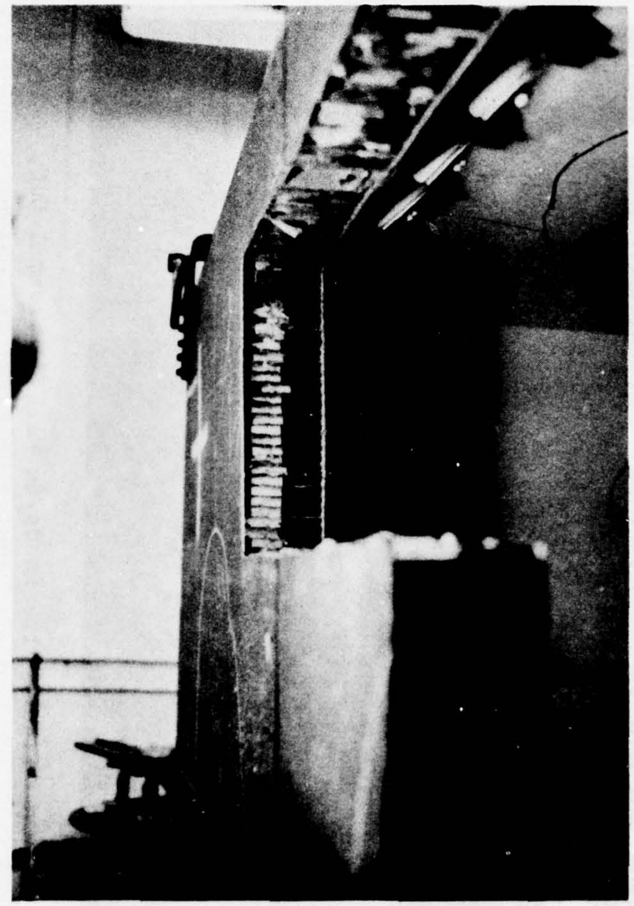

Figure 30. Horizontal Cut in Roadside Wall, View Toward Front End Wall

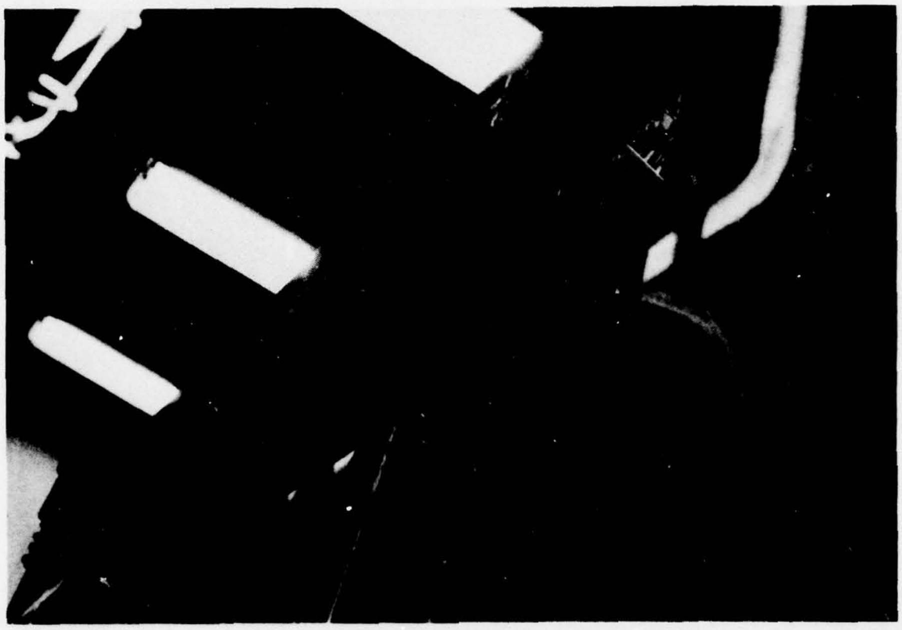

Figure 31. Roadside Wall Horizontal Cut, Showing Vertical Extrusion

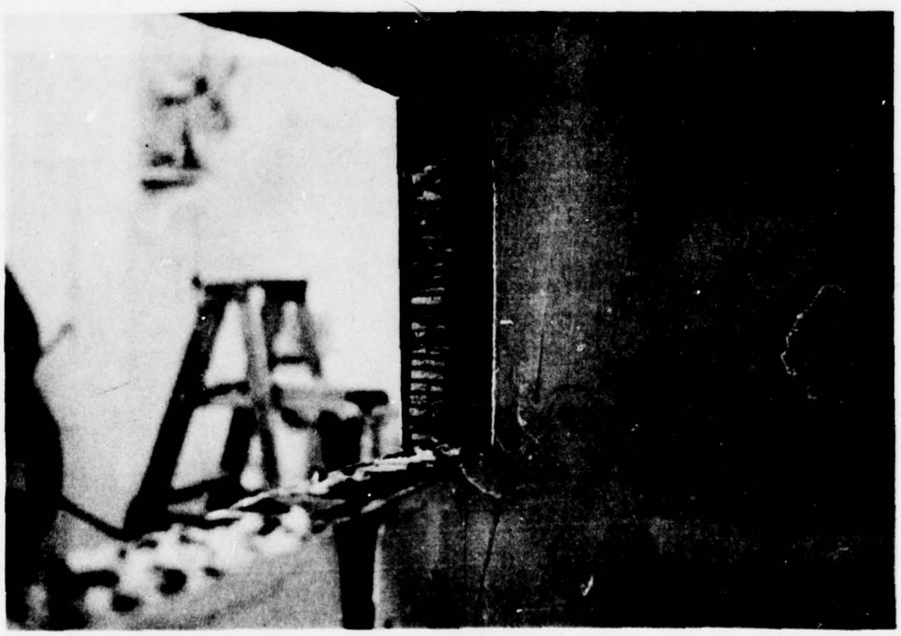

Figure 32. Interior View of Roadside Wall Cut

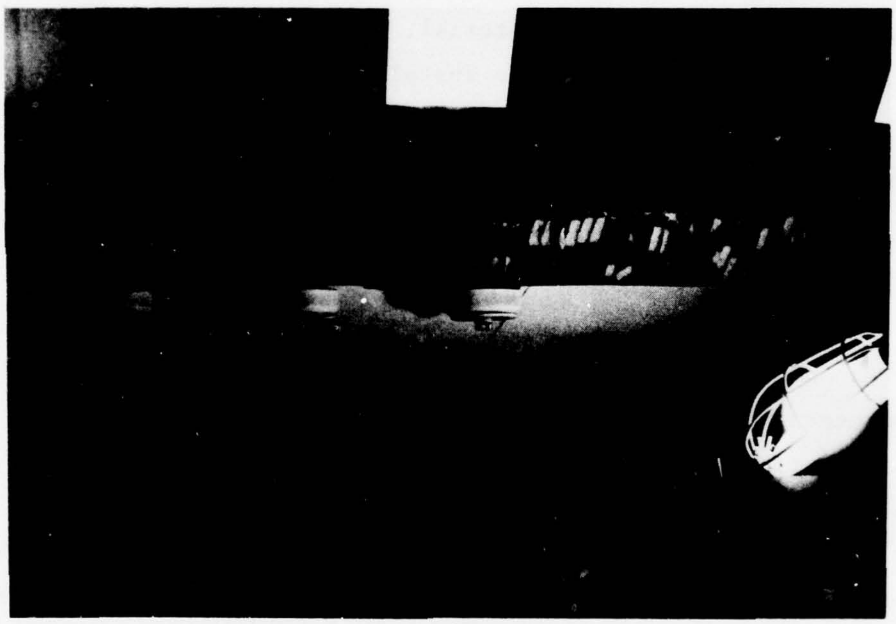

Figure 33. Exterior View of Horizontal Roadside Wall Cut, Showing Core Damage and Vertical Extrusion.

roadside wall is apparent in Figure 29. Delamination is seen in Figure 30, indicating the extent of this type of failure towards the center of the wall. This cut also confirmed the presence of the vertical extrusions (Figures 33 and 34). These extrusions were connected to the outside and inside facing sheets by rivets through the joint splices. In addition, one side of the extrusion was bonded to the outside facing sheets and the opposite side was bonded to a thermal barrier which, in turn, was bonded to the inside facing sheets. Foaming adhesive was inserted on the other two sides in contact with the honeycomb material. Figure 35 illustrates the cross-section of the extrusion installation.

Considerable internal damage resulted at the vertical extrusion (Figures 33 and 34). There was complete failure of the thermal barrier and the foaming adhesive, and extensive shear failure of the honeycomb core. The extrusion was also bent along its axis.

Figures 36, 37, 38, 39, 40 and 41 show the roof cut and corresponding core failures. A good indication of the roof deformation mentioned earlier, showing the edge depressions and the flat central region, is given in Figure 36. The internal failure in the roof cut (Figures 37, 38, 39, 40, 41 and 42) was clearly shear failure of the core near the panel edges due to the downward overpressure loading. The classical 45 degree shear failure planes are evident in the photographs. The shear failure was present on all faces of the roofside cut, away from the central flat portion where no failure of any type occurred. No delaminations were present as in the roadside cut. The foaming adhesive had failed at the curbside end of the roof cut. Figures 37, 38 and 41 show the shear deformation beginning along the edges of the upper shock-isolation mounts. A view of the section removed from the roof is shown in Figure 42.

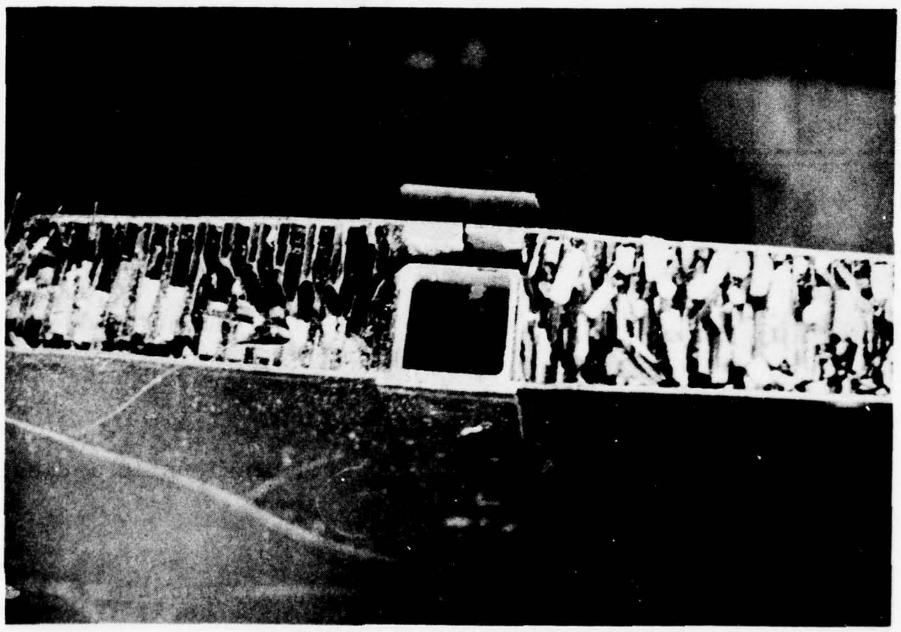

Figure 34. Vertical Extrusion in Roadside Wall, From Outside. Core Failure, Foaming Epoxy and Thermal Barrier.

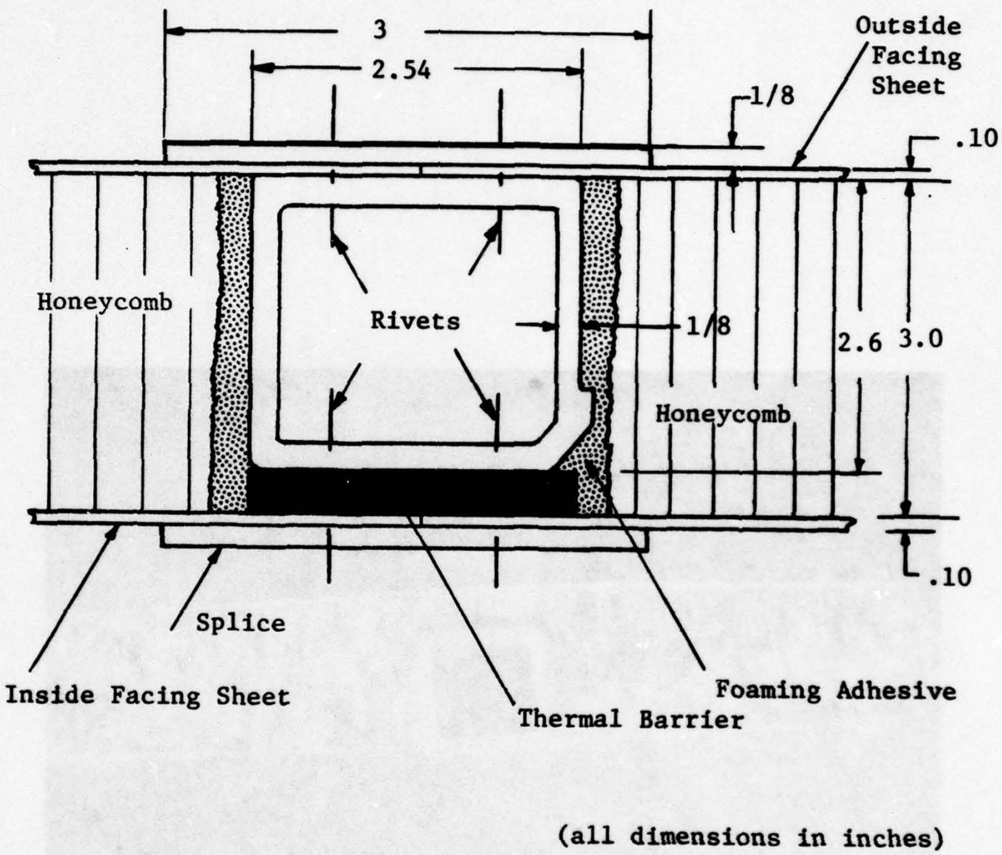

Figure 35. Vertical Extrusion Assembly in Roadside Wall

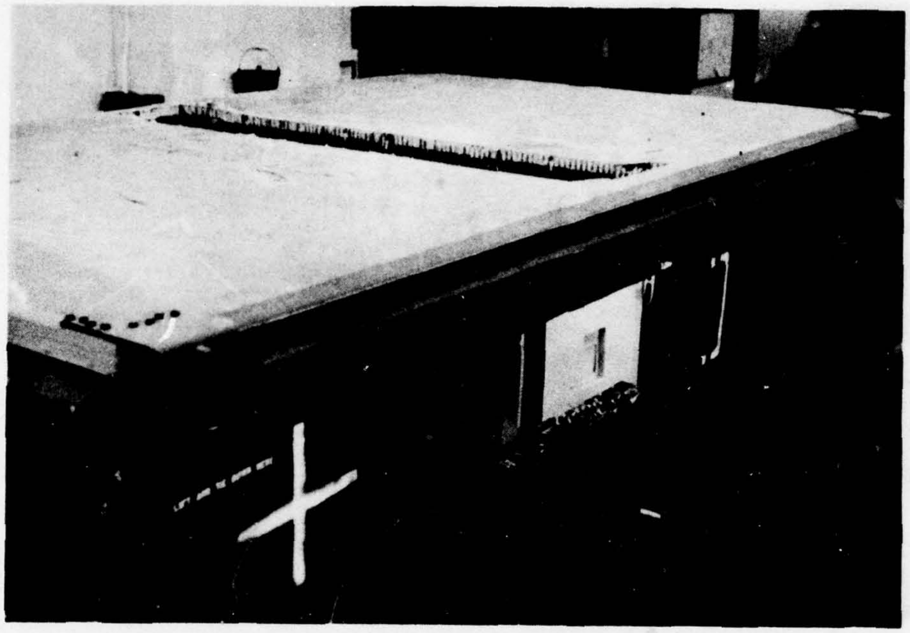

Figure 36. View of Roof and Roadside Wall Cuts

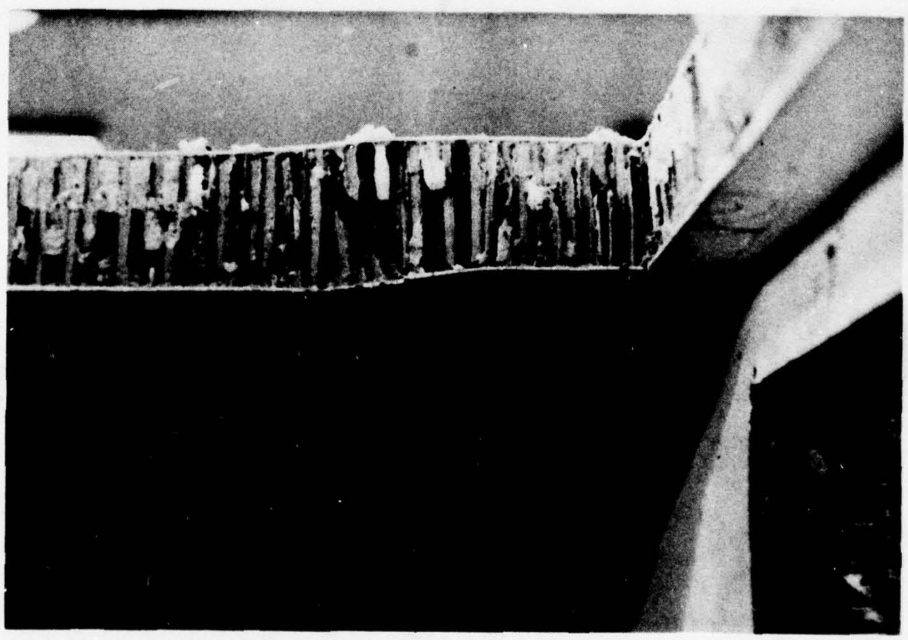

Figure 37. Roof Cut Near Curbside Wall, View Toward Front End Wall. Partial View of Curbside Cut

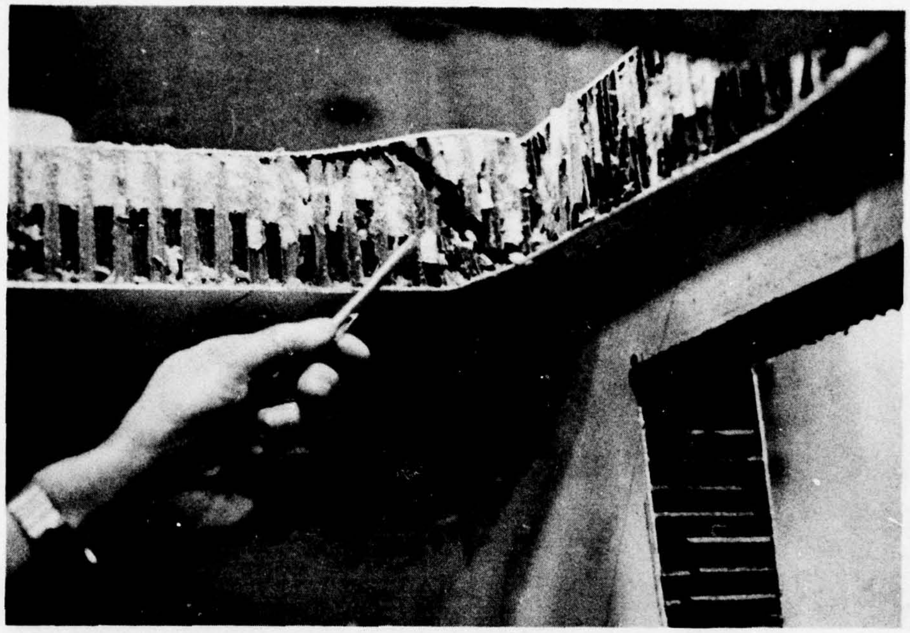

Figure 38. Roof Cut Near Roadside Wall, View Toward Door End Wall

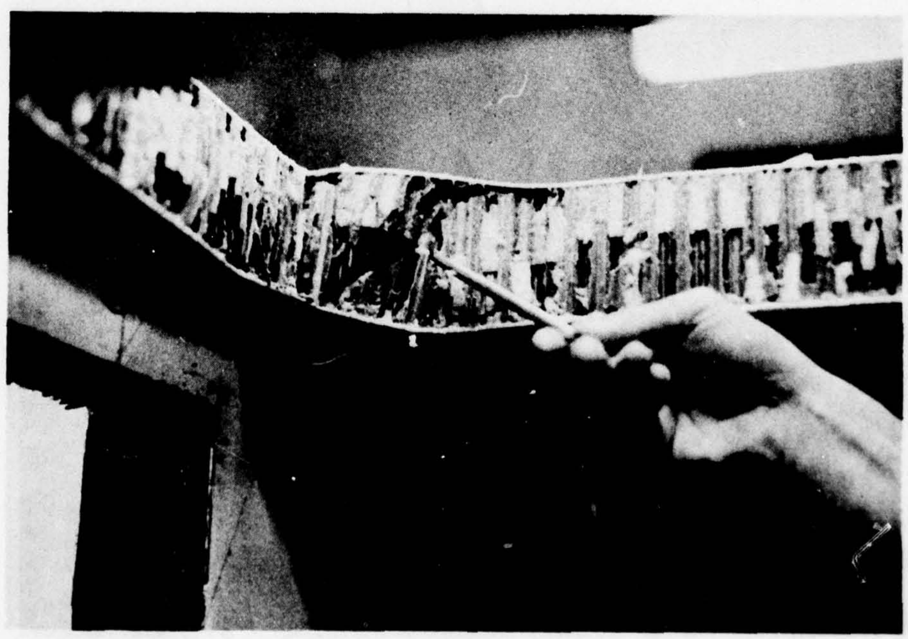

Figure 39. Roof Cut Near Roadside Wall, View Toward Front End Wall

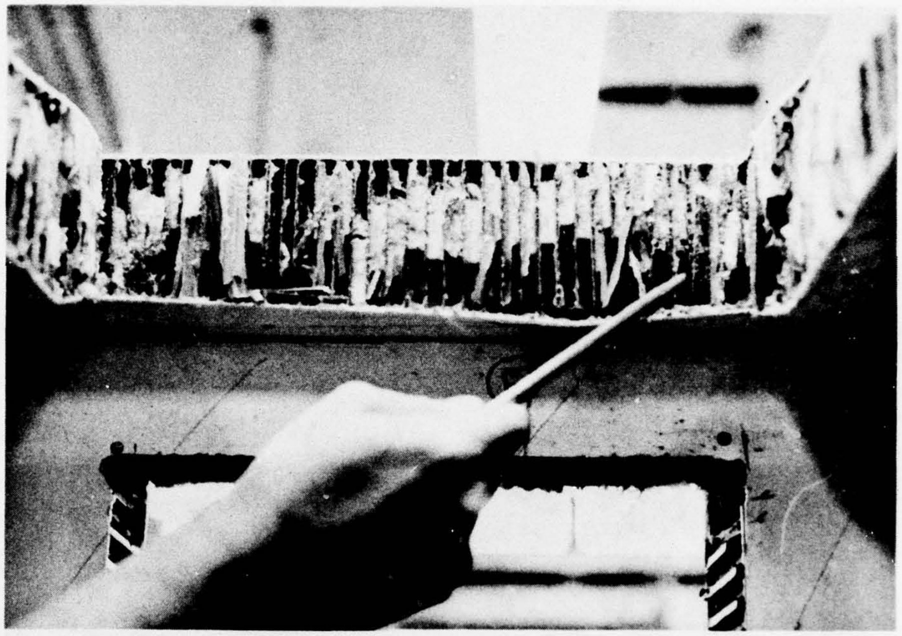

Figure 40. Roof Cut Near Roadside Wall, View Toward Roadside Wall

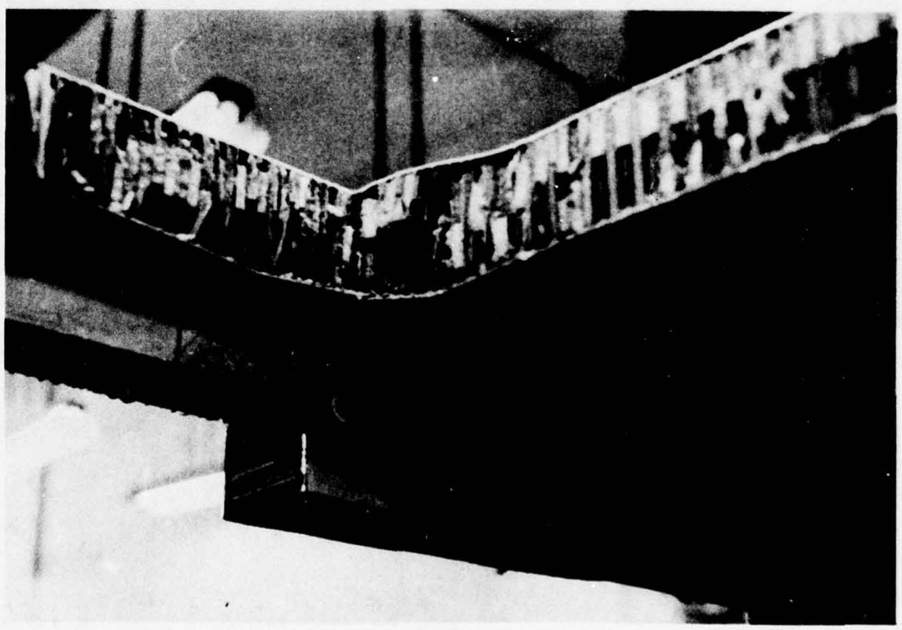

Figure 41. Roof Cut Near Roadside Wall, Showing Shear Deformation Along Edge

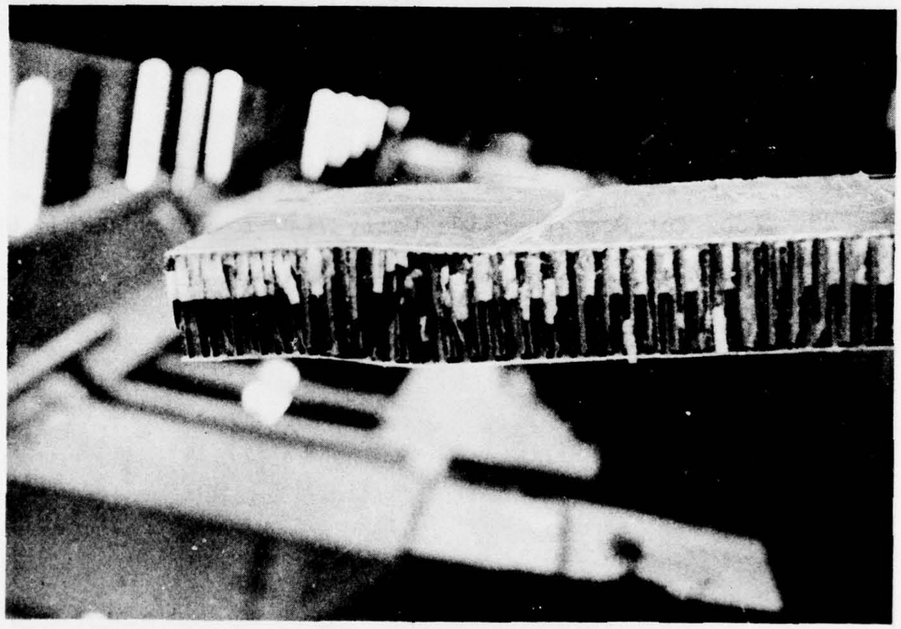

Figure 42. Section Removed from Roof

Failures in the curbside wall-cut are shown in Figures 43, 44, 45, 46 and 47. The upper surfaces of the cut showed shear failure of the core. Extensive core damage resulted at the upper part of the cut (Figure 45) as well as failure of the thermal barrier and the foaming adhesive. At the base of the cut and the sides, Figure 43, delamination occurred, again with some evidence of adhesive failure and core failure at the adhesive surface.

A portion of the edge extrusion above the roadside wall cut was also removed (Figure 48). The edge extrusion actually consists of two extrusions bolted together for modular construction. Shear failure of the foaming adhesive (dark region) and some cracking of the thermal barrier (light region) are apparent. Some shearing also is noticeable along the plane where the two extrusions are bolted.

More detailed photographs of the core shear failure are shown in Figure 49 (roadside edge of the roof cut) and Figure 50 (upper right-hand portion of the curbside road cut).

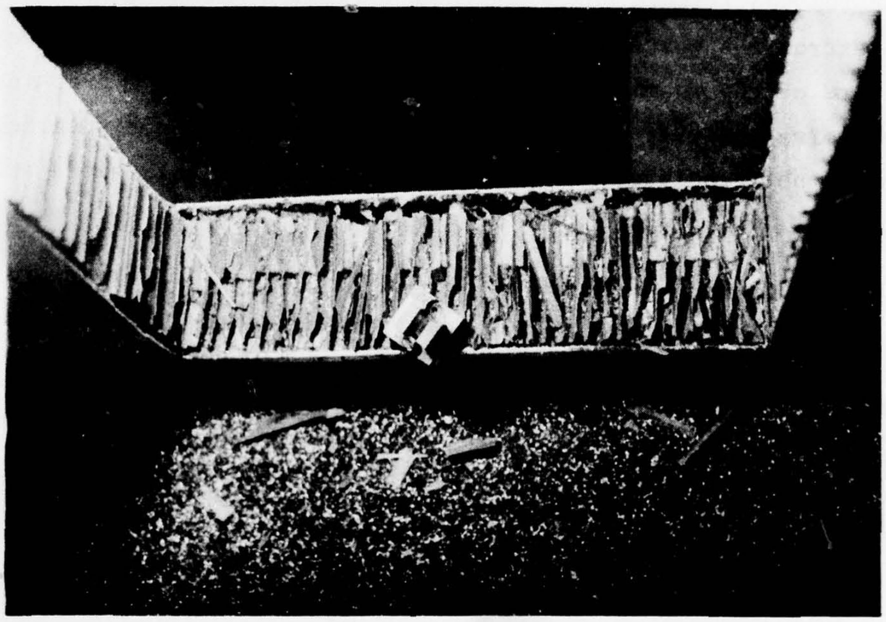

Figure 43. Interior View of Base of Curbside Wall Cut

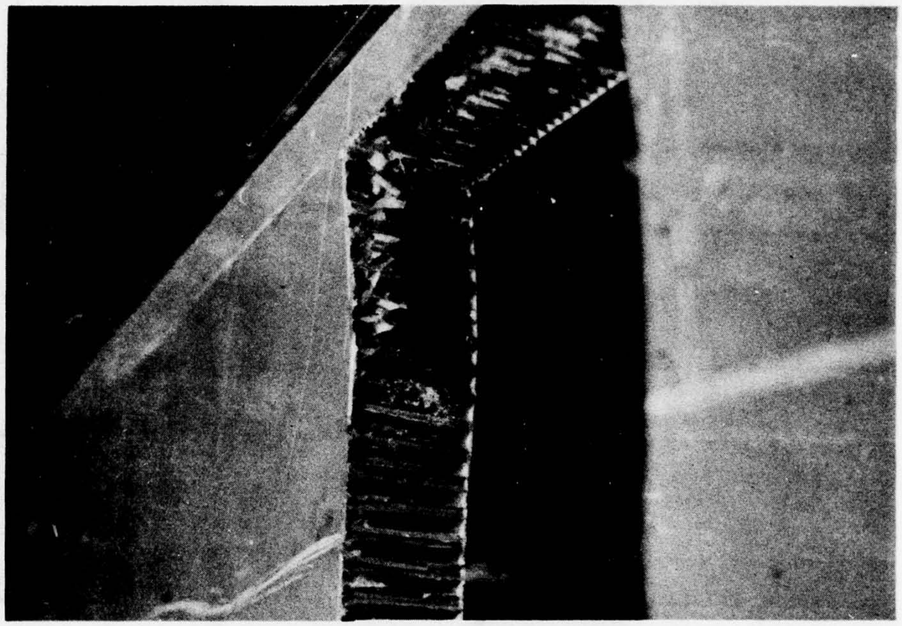

Figure 44. Curbside Wall Cut, Exterior View Toward Door End Wall

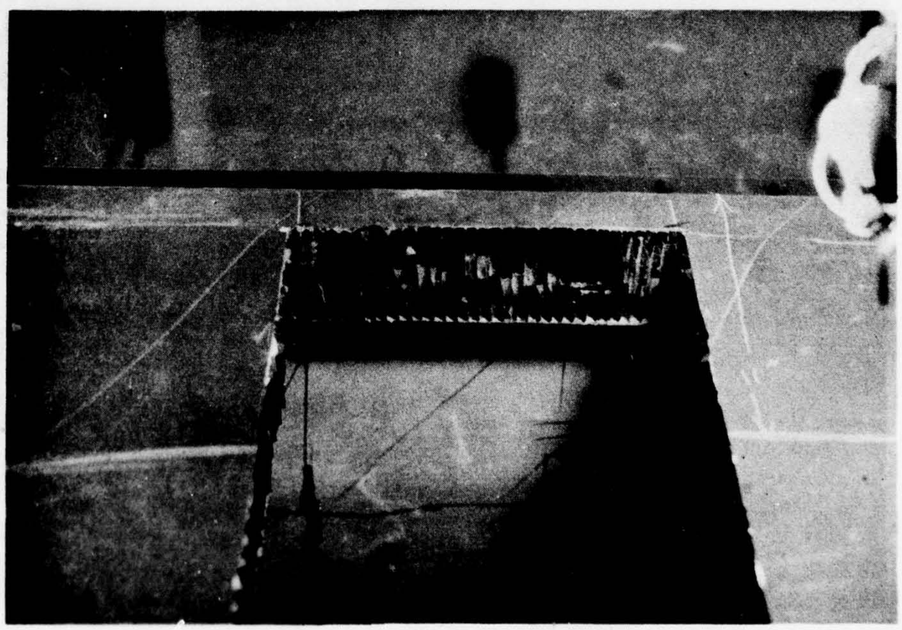

Figure 45. Upper Portion of Curbside Wall Cut

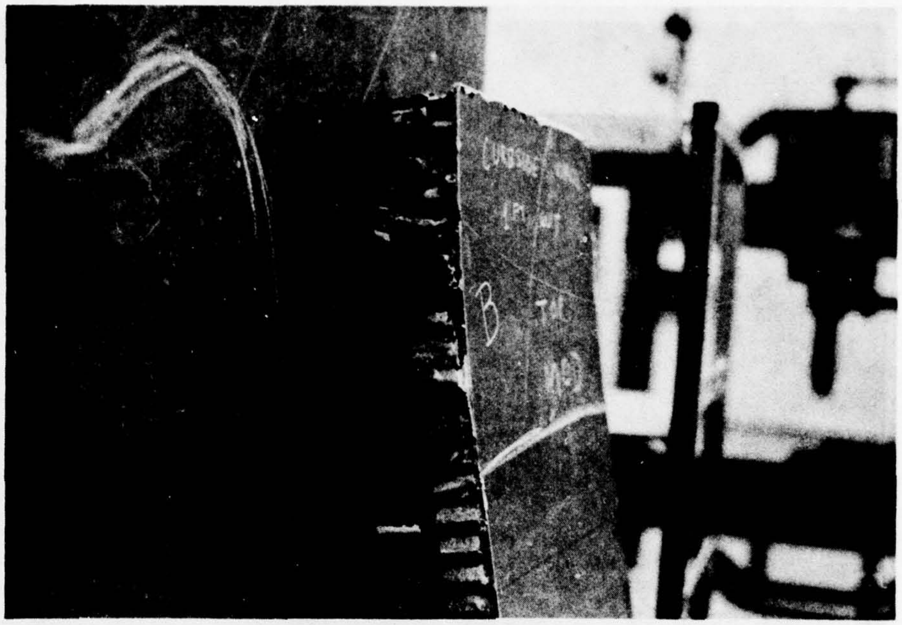

Figure 46. Upper Left Edge of Curbside Wall Cut

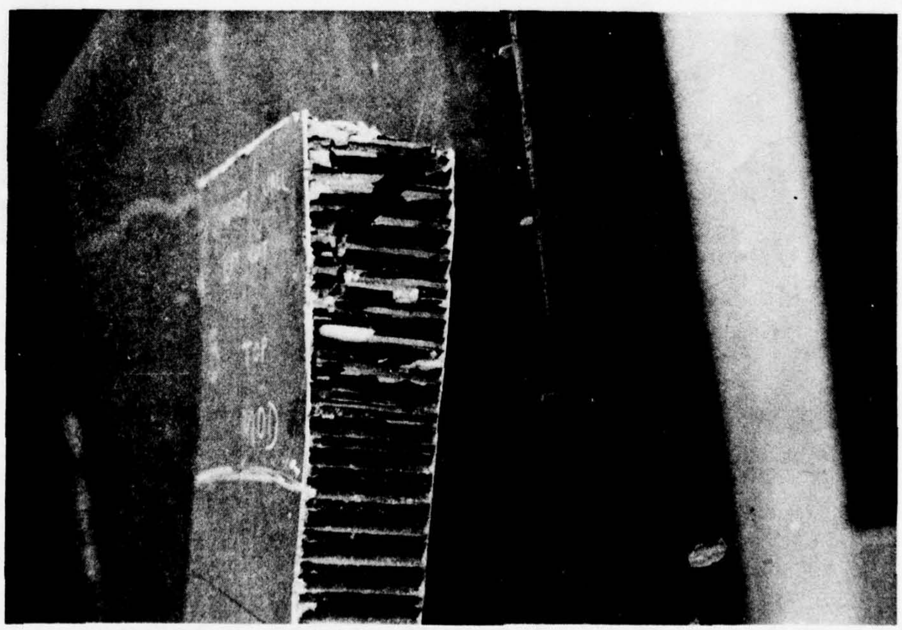

Figure 47. Upper Right Edge of Curbside Wall Cut

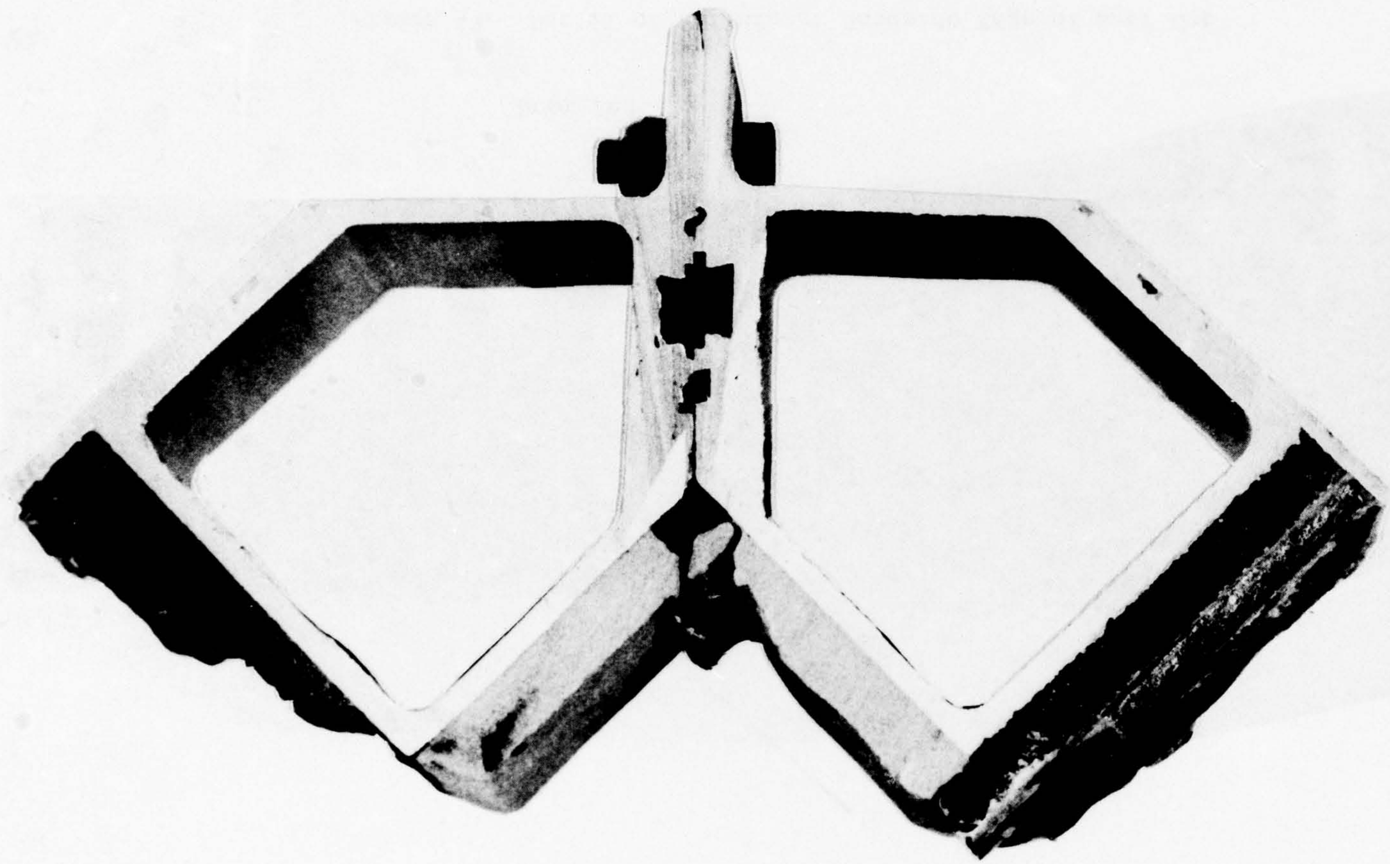

Figure 48. Section of Upper Edge Extrusion Removed From Roadside Wall

Roof

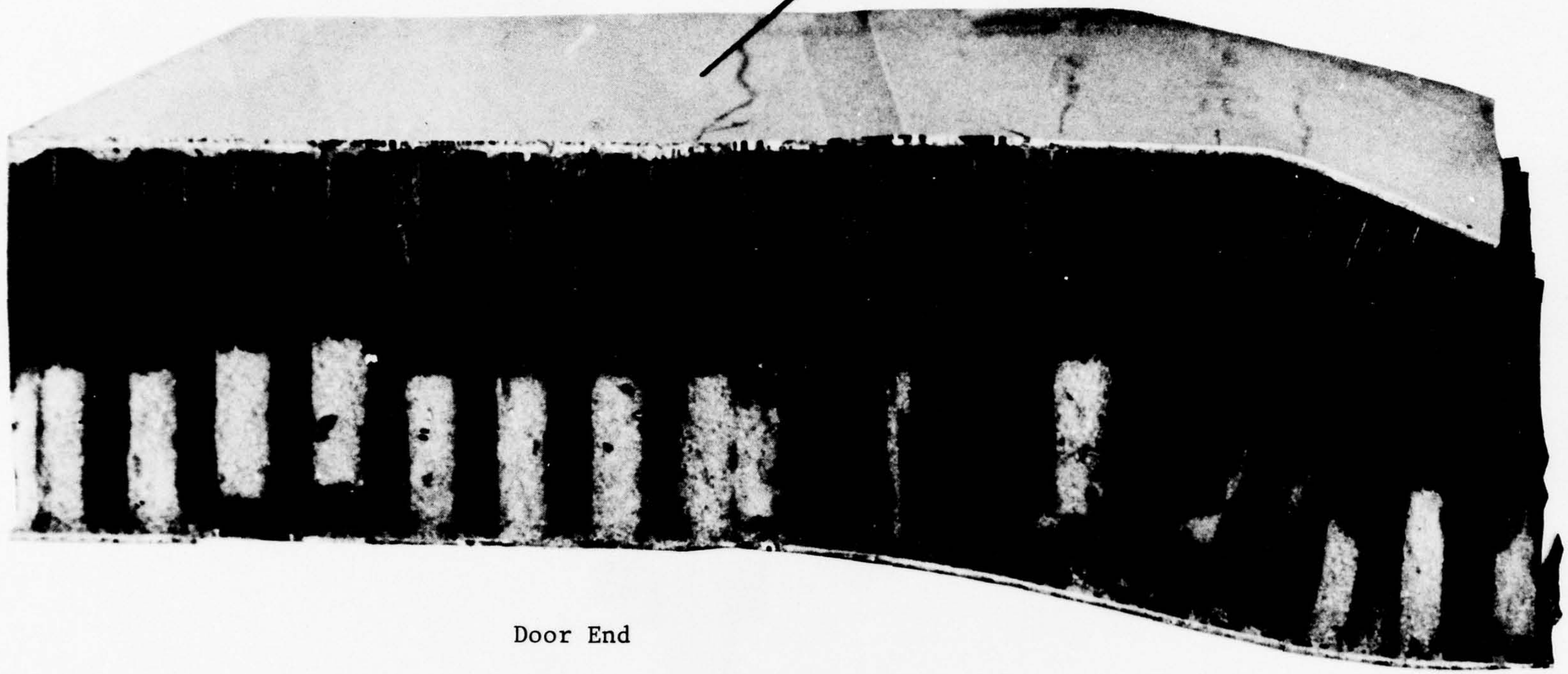

Door End

Figure 49. Detail of Failure at Roadside Edge of Roof Cut

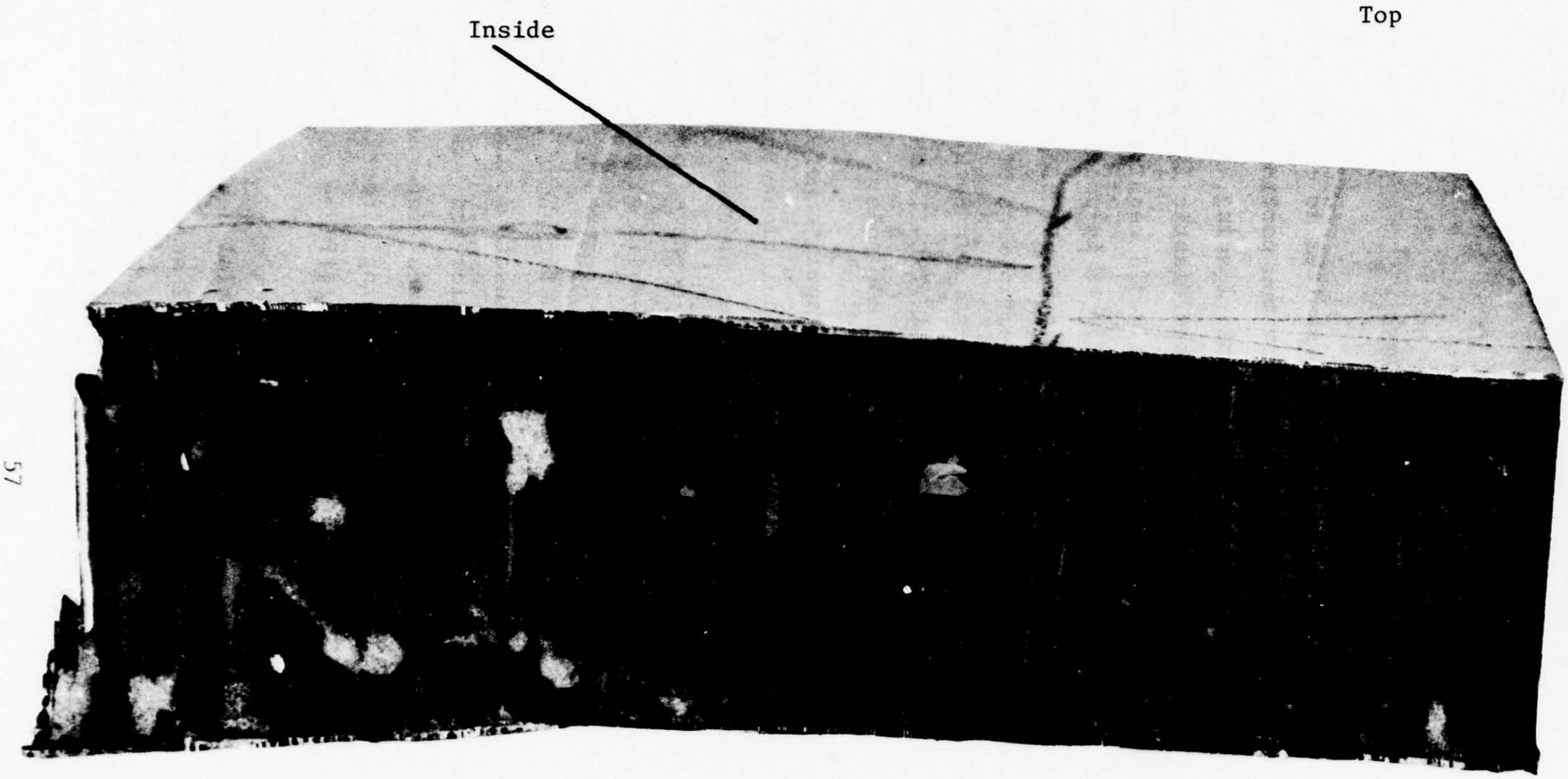

Figure 50. Detail of Failure at Upper Right Hand Portion of Curbside Road Cut

SECTION 5

STRESS CALCULATIONS

A dynamic stress analysis of the MOD shelter is complex because of the coupled interactions between the various portions of its structure, the nature of the applied dynamic loading, and the fact that the panel responses extended beyond the elastic limit of the facing material. An analysis such as this would require use of a large-scale structural finite element code. It is possible, however, to analyze a portion of the shelter, such as a wall panel, using the appropriate boundary conditions and descriptions of the mass, stiffness, and material stress-strain properties. Such an analysis has been done for the roadside wall of the AN/TRC-117 shelter in Ref. 6 for the nonlinear range using the DEPROP code.

Neither of these two approaches is appropriate here, for they are beyond the scope of this paper. The calculations presented here would be adequate for preliminary design purposes and the intent is to show that the structural failures that occurred are consistent with basic calculations. The basic method used is given in Ref. 7 and considers the nature of the sandwich construction of the walls, i.e., that the purpose of the core is to transfer shear to the metal facing sheets and the purpose of the facing sheets is to resist the bending stresses. As long as the core maintains its bond with the outer facing sheets and does not rupture or shear internally, it will provide a section modulus to resist bending effects. The shear contribution of the facings and the bending stiffness of the core are negligible.

The analysis assumes structural and material behavior in the linear elastic range and treats the wall panel as simply supported along all four edges. Calculations are made for the roof panel since the analysis cannot account for the presence of the roadside wall extrusions.

Referring to Figure 51 for definitions, the geometric and material properties of the roof panel, using 5052-H34 aluminum for the facings and WR II-3/8-3.8 paper honeycomb for the core, are

$t = 0.063$ in.	(Facing thickness)
$t_c = 3.0$ in.	(Core thickness)
$d = t_c + 2t = 3.126$ in.	
$a = 138.6$ in.	("W" direction)
$b = 83.3$ in.	("L" direction)
$b/a = 0.60$	
$G_{c_a} = 9{,}000$ psi	(Shear modulus in "W" direction)
$G_{c_b} = 19{,}000$ psi	(Shear modulus in "L" direction)
$E_f = 10 \times 10^6$ psi	(Youngs modulus for aluminum)
$\mu = 0.30$	(Poisson's ratio)

where the "L" direction corresponds to the ribbon direction and "W" to the panel length.

The bending-shear stiffness parameter V is, substituting the above data,

$$V = \frac{\pi^2 E_f \, t t_c}{2\,(1-\mu^2)\, b^2 \, G_{c_a}} = 0.164 \qquad (4)$$

The maximum bending moments occur at the panel center. With respect to the a and b axes these moments, in terms of the applied normal overpressure Δp, are

$$M_a = \frac{16\, b^2\, (C_3 + \mu C_2)\, \Delta p}{\pi^4}$$

$$(5)$$

$$M_b = \frac{16\, b^2\, (C_2 + C_3)\, \Delta p}{\pi^4}$$

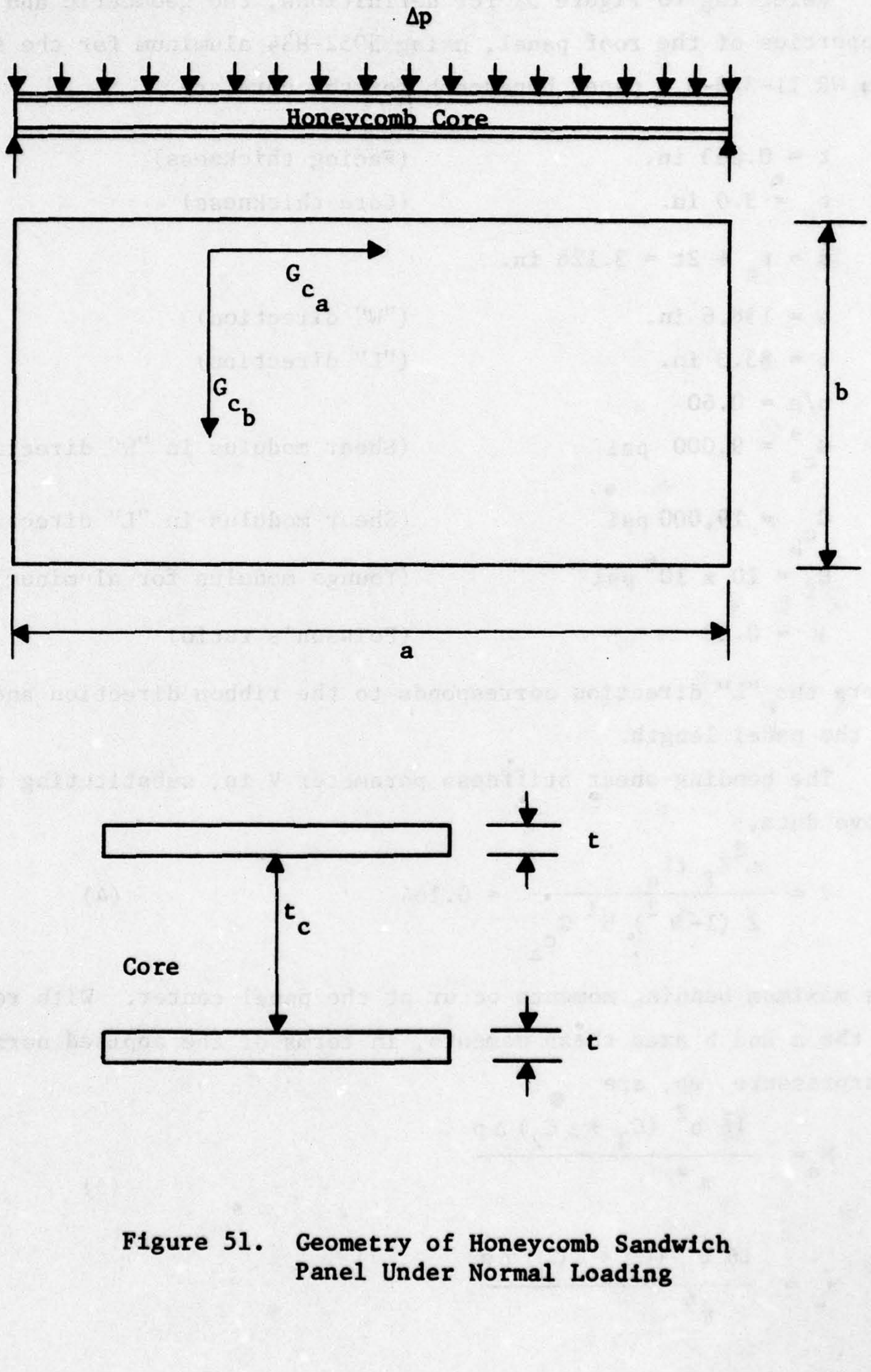

Figure 51. Geometry of Honeycomb Sandwich Panel Under Normal Loading

where the coefficients C_2 and C_3 are found from Ref. 7 in terms of the parameters V = 0.164 and b/a = 0.60 to be

$$C_2 = 0.52$$
$$C_3 = 0.14 \qquad (6)$$

Substituting into Eq (5), the maximum bending moments acting on the roof panel are

$$M_a = 337.4\ \Delta p \text{ in-lb/in}$$
$$M_b = 640.5\ \Delta p \text{ in-lb/in} \qquad (7)$$

and the corresponding stresses in the aluminum face sheets in terms of the overpressure are

$$\sigma_{f_a} = \frac{2\ M_a}{t\ (d + t_c)} = 1748\ \Delta p \text{ psi}$$

$$\sigma_{f_b} = \frac{2\ M_b}{t\ (d + t_c)} = 3319\ \Delta p \text{ psi} \qquad (8)$$

The maximum shear loads S_a and S_b occur at the midlength of the panel edges

$$S_a = \frac{16\ b\ C_4}{\pi^3}\ \Delta p$$
$$S_b = \frac{16\ b\ C_5}{\pi^3}\ \Delta p \qquad (9)$$

where the coefficients C_4 and C_5 are given in Ref. 7 in terms of the parameters V and b/a to be

$$C_4 = 0.85$$
$$C_5 = 0.70 \qquad (10)$$

The corresponding maximum shear stresses σ_{S_a} and σ_{S_b} in the honeycomb are

$$\sigma_{S_a} = \frac{2\ S_a}{d + t_c} = 12.1\ \Delta p \text{ psi}$$

$$\sigma_{S_b} = \frac{2\ S_b}{d + t_c} = 9.8\ \Delta p \text{ psi} \tag{11}$$

Thus far, the maximum stresses in the face sheets, Eq 8 , and the maximum shear stresses in the core, Eq 11 , have been expressed in terms of the applied overpressure on the roof, Δp. Referring to Section 3, the overpressure acting on the roof is approximately 7.0 psi, which will be reduced here by 25 percent to account for the rise time and shock traversal time across the roof to obtain an average value of 5.25 psi. Assuming a dynamic load factor of 2.0 because of the sudden application of the blast-induced roof load,

$$\Delta p = 5.25 \times 2.0 = 10.5 \text{ psi} \tag{12}$$

Substituting $\Delta p = 10.5$ psi into Eqs 8 and 9, the maximum facing stresses are

$$\sigma_{f_a} = 18{,}350 \text{ psi}$$

$$\sigma_{f_b} = 34{,}850 \text{ psi} \tag{13}$$

and the maximum shear stresses in the core are

$$\sigma_{S_a} = 127 \text{ psi}$$

$$\sigma_{S_b} = 103 \text{ psi} \tag{14}$$

The corresponding yield and ultimate stresses for the aluminum facings are approximately

$$\sigma_{Yield} = 31{,}000 \text{ psi}$$

$$\sigma_{Ult} = 38{,}000 \text{ psi} \tag{15}$$

and the corresponding allowable shear stresses for a 3-inch core are approximately

$$\left(\sigma_{S_a}\right)_{Allow} = 114 \text{ psi} \quad \text{(Ribbon Direction)}$$

$$\left(\sigma_{S_b}\right)_{Allow} = 78.4 \text{ psi} \quad \text{(W Direction)} \qquad (16)$$

The allowable shear stresses in Eq 16 include a reduction factor of 0.70 for core thickness and a reduction factor of 0.80 for dynamic effects as recommended by Hexcel.

Comparing the estimated maximum stresses in Eqs 13 and 14 with the corresponding allowable stresses in Eqs 15 and 16, it is seen that the face sheets are predicted to yield in tension and the core is predicted to fail in shear. The above calculations were verified independently by the method of Ref. 8. Since the geometry (b/a) and cross-section of the curbside wall are essentially the same as for the roof, the above calculations would also predict the same panel failures for the curbside wall.

The shear forces on the roadside (blast side) wall would be greater than those on the roof because the applied overpressure is significantly greater (Fig. 8 compared to Fig. 9). Therefore the roadside wall would also be expected to fail in shear. With regard to the bending stresses in the roadside wall, it was seen that considerable core shear failure occurred at the vertical stiffening extrusion. Therefore the stiffener at some point in time became ineffective in resisting the bending stresses because of failure in the shear transfer mechanism. Assuming the stiffener to be completely ineffective in reducing the panel bending stresses, the maximum panel bending stresses calculated by the above procedure would be 65,000 psi for the roadside wall. The stiffener obviously provided some bending resistance for the panel, but not to the extent where the 65,000 psi level would be reduced to below the yield stress of 31,000 psi. With this reasoning, yielding of the facing sheet on the roadside wall would also be anticipated.

The effect of increasing the core thickness t_c from 3.0 inches to 4.0 inches, while maintaining the other data constant, was also investigated. It was found that the maximum stresses in the facings were reduced to

$$\sigma_{f_a} = 13{,}840 \text{ psi}$$

$$\sigma_{f_b} = 26{,}274 \text{ psi} \qquad (17)$$

Similarly the maximum shear stresses in the core were reduced to

$$\sigma_{S_a} = 96 \text{ psi}$$

$$\sigma_{S_b} = 77 \text{ psi} \qquad (18)$$

Increasing the core thickness to 4.0 inches would thus reduce the stress levels below the corresponding allowable values in Eqs 15 and 16.

It should be emphasized again that the above stress calculations are approximate and are of a nature that is adequate primarily for preliminary design purposes. However, they do point to the failures that were ultimately experienced during the test.

In designing the MOD shelter, the dynamic nature of the applied overpressure loading was neglected by the manufacturer. In addition, due to a misunderstanding, a peak overpressure of 7.3 psi was used for the applied loading on the roadside wall instead of the reflected overpressure of 15.7 psi (Eq 2). As a result, the design loads for the MOD shelter were underestimated, by approximately a factor of four for the roadside wall and a factor of two for the roof and curbside wall.

During fabrication, an attempt was made to correct for the oversight in the reflected overpressure by increasing the facing thicknesses of the roadside wall from the original 0.063 inch to 0.10 inch and by adding the two vertical extrusions. These modifications, however, increased the overall bending strength of the roadside wall but did not noticeably increase its shear strength. As a result, shear rupture of the core was a major mode of failure for the roadside wall.

SECTION 6

SUMMARY OF FINDINGS AND RECOMMENDATIONS

A post-test analysis was made of the structural damage incurred by the Brunswick MOD shelter in the DICE THROW HE blast test conducted in October 1976 at the White Sands Missile Range. The MOD shelter was of modular design using a special-application Hexcel paper honeycomb, WR II-3/8-3.8, for the core material of the wall panels.

Although the intent of the MOD shelter was to survive a 7.3-psi incident overpressure, the roadside wall, which received the shock wave broadside, was designed without accounting for the reflected nature of the incident shock. In addition, the dynamic nature of the applied loading was not included in the structural design of the wall and roof panels. Thus, the MOD shelter was subjected to considerably higher blast loads than anticipated, an important consideration in the damage assessment.

The shelter is of interest to the GLCM program basically because of the paper-honeycomb-core concept, the structural framing, the adhesives, seals, construction techniques used, and the equipment rack configuration. In addition, its condition after being in the field for an extended period of time provides some insight into the weatherability of the modular design.

6.1 Summary of Major Findings

The overall post-test condition of the shelter was examined, measured, and photographed; structural panel sections were removed and carefully studied; and approximate stress calculations were made. A summary of the major findings of this post-test analysis is as follows:

- The roadside wall, roof and curbside wall were permanently deformed or dished-in. The maximum panel deformations were of the order of two inches normal to their planes. There was none of the wrinkling or creasing on the skin facings observed on blast-damaged S-280 shelters. The deformation of the roadside wall was bi-concave in form; the roof and curbside walls were depressed only near their edges with fairly flat central regions.
- There was no damage to either the door-end wall or the opposite (front-end) wall. The epoxy filler in the door frame had cracked but the door frame appeared undamaged. Some delamination had occurred in the door panel.
- The edge extrusions to which the wall panels were connected appeared undamaged and displayed no permanent overall bending deformations.
- There were no tears, ruptures or other catastrophic failures of the exterior structure of the shelter, thus implying that protection against EMP and CBR* was unaffected, except perhaps, where several rivets had popped from the vertical roadside extrusions. However, there was sufficient structural weakening to imply that the shelter could not be expected to survive a subsequent blast of any significant magnitude. It is very likely that further damage would result in a loss of the EMP and CBR protection.
- The exterior of the shelter was in very good condition considering that it had been blast-tested and subsequently exposed to the weather for two years. There was no evidence of any water penetration into the honeycomb core or the shelter interior.

---

*Electromagnetic pulse and chemical-biological-radiation.

- The roadside wall racks sustained serious damage from impact with the wall and roof. The curbside wall racks were also impacted by the roof but not by the adjacent wall. The top shock mounting-blocks remained bolted to the top edge extrusions as opposed to the mounting blocks in the BRL retrofit shelter, which lost their adhesive bond during the test.

- The overall damage to the MOD shelter was significantly less than the damage incurred by the AN/TRC-117's S-280 shelter, which was located at the same blast line. A comparison must consider, however, that the S-280 has thinner skins, weaker edge beams, and a significantly weaker polyurethane core; in addition, it was not designed for blast loads.

- The wall panels failed internally as a result of shear failure of the core and also as a result of separation of the core from the aluminum facings. This separation was due to either failure of the core material at the adhesive surface or to failure of the adhesive at the facing surface. The shear failure occurred characteristically near extrusion edges. Delamination failure also occurred near extrusion edges and extended, in some cases, significantly toward the central regions of the panels.

- The foaming adhesive and the thermal barrier failed at the edge extrusions and at the vertical stiffeners in the roadside wall.

- The effectiveness of the vertical stiffeners in the roadside wall cannot be fully determined since there was considerable failure of the honeycomb and the thermal barrier near the stiffener. As a result of this failure, the load transfer between the wall panel and stiffener was greatly diminished. The bi-concave-like deformation shape of this wall is most likely attributed to the bending stiffness of the thicker roadside facings, with some contribution from the two vertical stiffeners.

- The approximate stress calculations presented herein predict that yielding of the core facings and shear failure of the core would occur in the roadside, roof and curbside walls and correlate with the observed failures.

6.2 Conclusions

- A major conclusion of this effort is that the WR II-3/8-3.8 paper honeycomb core is highly suspect as a candidate material for wall panels that may be subjected to an overpressure environment of approximately six to seven psi. DICE THROW has demonstrated that wall and roof panels using this core material are susceptible to shear failure in this overpressure range. Increasing the core thickness could result in somewhat lower shear stresses, as shown herein, but impractical wall thicknesses may result.

- The foaming adhesive proved to be inadequate and the structural adhesive marginally adequate. Failure of both adhesives contributed to overall panel failure.

- The panel-edge extrusion proved successful, displaying no failures or permanent bending deformations. However, attachment of only one of the two facing sheets of a panel directly to an edge extrusion (with the other skin bonded to a thermal barrier) allowed some failures along the edges of panels. A more secure means of fastening the facing sheets to the extrusions should be implemented.

- The sealants were very effective and were not degraded by the blast. The shelter sustained the elements very well for two years following the blast test. A full assessment of the sealants cannot be made for GLCM application, however, since the shelter remained stationary during this time and the sealants and joints were not subjected to the vibratory stresses associated with road mobility.
- The equipment rack structure is not adequate for a dynamic blast environment. A more substantial framing design would be necessary.
- The effectiveness of the rack isolation system cannot be evaluated since the racks did not support electronic equipment or simulated weights during the test.
- In general, the modular panel design was proven under the blast loading, the shelter retaining its structural integrity. However, the design's suitability for GLCM application will depend on its ability to include an armor-piercing-incendiary (API) protection concept, one form of which might be a field-installed API kit.

6.3 Recommendations

- It is recommended that blast tests, such as shock tube tests, be conducted on any structural panel candidates under consideration for the GLCM shelter prior to design selection. These tests could be conducted by either the contractor or BRL and would demonstrate the candidate panel's ability to withstand sequential applications of the specified overpressure without skin yield, core damage, adhesive failure, joint connectivity failure, or other modes of failure. The tests should be conducted on panels sufficiently large to be representative of a shelter wall.

Additional GLCM design requirements dictated by other specified environments, such as API, EMP, CBR, thermal, etc. must also be considered concurrently.

- A shock-isolation system has already been proposed for the GLCM equipment racks. Prior to design implementation, experimental work is needed to assess the adequacy of this system in protecting not only against blast loads, but also against the non-hostile shock environment and the potentially damaging vibratory motions induced by road mobility.

- The analytical methodology must account realistically for both the nature of the dynamic overpressure loading on the GLCM shelter and the assembled structural detail of the shelter itself, and should be more comprehensive than the stress analysis presented herein.

APPENDIX

FUNDAMENTAL PANEL FREQUENCY

The fundamental (lowest) natural frequency ω_1 of the roof or curbside wall panels may be calculated by the method of Ref. 9. Neglecting shear effects of the core and the rotary inertia of the two facings, the fundamental frequency is

$$\omega_1 = \frac{\pi^2}{b^2}\left[1 + \left(\frac{b}{a}\right)^2\right]\sqrt{\frac{Dg}{(1 + t/t_c)\rho_t}} \qquad \text{A-1}$$

where D is the panel bending stiffness

$$D = \frac{E_f\ t\ t_c^2\ (1 + \frac{t}{t_c})^2}{2\ (1-\mu^2)} \qquad \text{A-2}$$

and ρ_t the panel density

$$\rho_t = 2\ \rho_f\ t + \rho_c\ t_c \qquad \text{A-3}$$

Substituting

$\frac{b}{a} = 0.60$

$b = 83.3$ in

$g = 386$ in/sec^2

$t = .063$ in.

$t_c = 3.0$ in.

$E_f = 10 \times 10^6$ psi

$\rho_f = 0.10$ lb/in^3

$\rho_c = 3.8$ lb/ft^3 $= 2.2 \times 10^{-3}$ lb/in^3

$\mu = 0.30$

the panel bending stiffness D is

$$D = 3.25 \times 10^6 \ \frac{\text{lb-in}^2}{\text{in}}$$

and the lowest panel frequency is

$$\omega_1 = 489 \text{ rad/sec} = 77.9 \text{ cps}$$

The correspond period of vibration is

$$\tau = \frac{1}{\omega_1} = 12.8 \text{ msecs}$$

With the effects of shear and rotary inertia included, the method of Ref. 9 gives, using more complicated mathematical relationships which are not reproduced here,

$$\omega_1 = 73.9 \text{ cps}$$

Therefore, these effects are negligible with regards to the lowest mode. The rotary inertia effect, however, will be more significant for the higher vibratory modes.

REFERENCES

1. Proceedings of the DICE THROW Symposium, 21-23 June 1977, DNA 4377P-1, Vol 1, Contract No. DNA 001-75-C-0023.

2. Mechanical Properties of Hexcel Honeycomb Materials, TSB 120, 1978 Edition, Hexcel, Dublin, California.

3. Harris & Creed, Shock and Vibration Handbook, page 49-7, McGraw-Hill Book Co , Inc., 1961.

4. Calligeros, J.M., Walsh, J.P. and Yeghiayan, R. P., Structural Modeling and Response of Command, Control and Communication Shelter Systems for Event DICE THROW, Kaman AviDyne KA TR-151, May 1978.

5. Lottero, Richard E, Computational Predictions of Shock Diffraction Loading on an S-280 Electrical Equipment Shelter, BRL MR 2599, March 1976.

6. Calligeros, J.M., Mente, L.J., Lee, W. N., Zartarian, G., Pre-Test Response Analysis of the AN/TRC-117 Shelter/Truck and AN/TRA-37 Antenna to the Blast Environment in MISERS BLUFF, (Interim Report), Kaman AviDyne Report KA TM-117, Sept. 1978.

7. Design Handbook for Honeycomb Sandwich Structures, Hexcel TSB 123, March 1970.

8. MIL HDBK-23A, Structural Sandwich Composites, 30 Dec. 1968, Department of Defense, Wash. D.C. 20025.

9. Chang, C.C. and Fang, B.T., Transient and Period Response of a Loaded Sandwich Panel, Journal of the Aerospace Sciences, Vol. 28, No. 5, May 1961.